8-2007

Glycosaminoglycan Stabilization Reduces Tissue Buckling in Bioprosthetic Heart Valves

Sagar Shah
Clemson University, sshah@clemson.edu

GLYCOSAMINOGLYCAN STABILIZATION REDUCES TISSUE BUCKLING IN BIOPROSTHETIC HEART VALVES

A Thesis
Presented to
the Graduate School of
Clemson University

In Partial Fulfillment
of the Requirements for the Degree
Master of Science
Bioengineering

---

by
Sagar Ramesh Shah
August 2007

Accepted by:
Dr. Naren R. Vyavahare, Committee Chair
Dr. Dan T. Simionescu
Dr. Jiro Nagatomi

ABSTRACT

Currently, bioprosthetic heart valves are crosslinked with glutaraldehyde to prevent tissue degradation and to reduce tissue antigenicity. Glutaraldehyde forms stable crosslinks with collagen via a Schiff base reaction of the aldehyde with an amine group of the hydroxylysine/lysine in collagen. However, within a decade of implantation, 20-30% of these bioprostheses will become dysfunctional and over 50% will fail due to degeneration within 12-15 years post-operatively [1, 2].

Gylcosaminoglycans, a major constituent of valvular tissue, play an important role in maintaining a hydrated environment necessary for absorbing compressive loads, modulating shear stresses, and resisting tissue buckling. One of the disadvantages of glutaraldehyde crosslinking is its incomplete stabilization of GAGs [3, 4], which lack the amine functionalities necessary for fixation by aldehyde addition. Previous studies have reported a greater depth of buckling in glutaraldehyde crosslinked aortic valves, one of the major causes of failure in these bioprostheses [5, 6]. Buckling occurs at sites of sharp bending, producing large stresses that can eventually lead to mechanical fatigue and consequent valvular degeneration. Local structural collapse occurs at these areas of tissue buckling to minimize compressive stresses, which subsequently causes a reduction in tissue length.

Previous studies have reported the loss of GAGs in glutaraldehyde crosslinked porcine cusps during fixation, storage, *in vitro* fatigue experimentation, and *in vivo* subdermal implantation due to enzyme-mediated GAG degradation [3, 4, 7, 8].

Additionally, GAG loss has been observed in failed porcine bioprosthetic heart valves following clinical use [9].

Therefore, to evaluate the potential role of GAGs in reduction of buckling in bioprosthetic heart valves, we used two 1-ethyl-3-(3-dimethylaminopropyl) carbodiimide (EDC) based crosslinking chemistries that link GAG carboxyl groups to the amine groups of proteins. Neomycin trisulfate, a hyaluronidase inhibitor, was employed to effectively stabilize the GAGs and subsequently prevent its enzymatic degradation. Previously, stabilization of valvular GAGs using neomycin trisulfate, a GAG-enzyme inhibitor, coupled with carbodiimide fixation chemistry was found to resist *in vitro* and *in vivo* enzymatic degradation of GAGs [10]. Thus, using the above-mentioned GAG-targeted fixation strategies, we demonstrate that the retention of valvular GAGs reduces the extent of buckling in bioprosthetic heart valves, which may subsequently improve the durability of these bioprostheses.

DEDICATION

To Clemson University for defining, directing and guiding me,

To the Tiger family – faculties, administrators, staff, and peers

for advising and leading me to that shining horizon of opportunities.

To my parents, Ramesh and Jayshree, and sisters, Sonal and Rupal,

for the millions of sacrifices that they continue to make,

for believing in me, and

for holding my hand,

every step of the way – always.

I owe my successes, accomplishments, and experiences to these selfless people….

ACKNOWLEDGEMENTS

I wish to extend my deepest appreciation to my mentor, advisor, and professor, Dr. Narendra R. Vyavahare. His continued encouragement, guidance, and support through the tenure of this study have enabled me to gain valuable knowledge and understanding of the field of bioengineering. These words do not give fair justice to the time and commitment that Dr. Vyavahare devoted to the betterment of my future. He inspired me to set the bar higher every step of the way – to aspire for that which may seem impossible or beyond reach, but is yet possible and can be pursued with enthusiasm and compassion.

I wish to express my sincere appreciation to my committee members, Dr. Dan T. Simionescu and Dr. Jiro Nagatomi, for their continued guidance, advice, and valuable insight.

Thanks to Mrs. Linda Jenkins for access to the departmental histology facility, Dr. Jason Isenburg and Dr. Lawrence Grimes for assistance with statistical analyses of results, and Mr. Darryl Krueger for guidance with Scanning Electron Microscopy imaging of samples. I am highly appreciative to my fellow colleagues in the Cardiovascular Implant Research Laboratory, especially Devanathan Raghavan and Lauren Browne for their kindness, assistance, and support, and Jeremy J. Mercuri for assistance and guidance during the initial stages of this research.

My deepest gratitude is reserved for the Department of Bioengineering (especially Dr. Martine LaBerge and Dr. Robert A. Latour) and the Department of Biological

Sciences (especially Dr. Alfred P. ‘Hap’ Wheeler) for affording me this opportunity to pursue this newly established 5-year BS/MS program.

Much thanks to Snow Creek Meat Processing Plant for access to porcine aortic heart valves. This study was supported by NIH (HL70969).

TABLE OF CONTENTS

Table of Contents (continued)

Page

Table of Contents (continued)

Page

LIST OF TABLES

LIST OF FIGURES

List of Figures (continued)

Figure **Page**

CHAPTER 1

LITERATURE REVIEW

1.1 Morphology of Heart Valves

1.1.1 Function

The heart, a hollow muscular organ located between the lungs and above the diaphragm, furnishes the power to maintain blood flow throughout both the pulmonary and systemic circulatory systems via its pulsatile pumping action [11]. Blood flow through the four chambers of the heart is controlled by the presence of heart valves; two atrioventricular valves (AV) situated between the atrial and ventricular chambers and two semilunar valves located between the ventricles and the aorta and pulmonary artery (**Figure 1**).

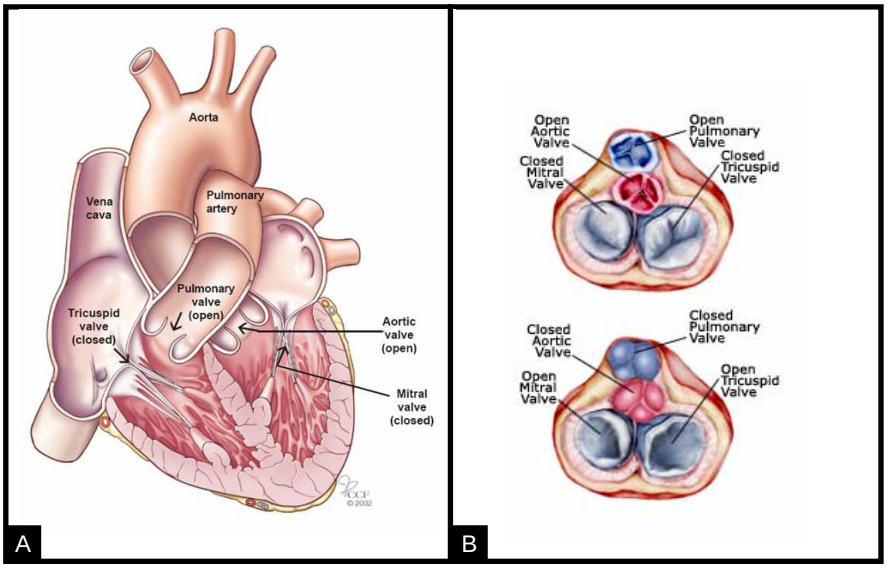

Figure 1: Cross-section of the (A) heart [12] and (B) valves [11].

The AV valves (the tricuspid and mitral valves) prevent backflow of blood from the ventricles to the atria during systole, ensuring the one-way flow of blood. During systole, ventricular contraction raises intraventricular pressure, causing the AV valves to passively close due to the pressure gradient. In parallel, the aortic and pulmonary valves, classified as semilunar valves, open to facilitate the onset of systemic circulation. These semilunar valves prevent backflow from the arterial vessels into the ventricles during diastole, allowing rapid filling of the ventricular chambers. As the ventricular pressure rapidly increases, the blood is ejected into the arterial vessels. Subsequently, the high pressures in the arteries at the end of the systolic phase of the cardiac cycle forces these valves to snap to the closed position. Thus, due to the rapid closure of the semilunar valves and forceful ejection of blood, the edges of these valves are continuously subjected to mechanical abrasion. Unlike the presence of a series of cord-like tendons attached to the vanes of the AV valves, the semilunar valves lack such structural support systems. These chordae tendineae prevent AV valves from bulging too far backward towards the atria during ventricular contraction. Thus, based on the anatomy of these valves, it is evident that semilunar valves must withstand extra physical stresses. The thin, filmy AV valves require minimal backflow to elicit valvular closure, whereas the heavier, robust semilunar valves demand rapid backflow for a few milliseconds [13]. Pulmonary valvular cusps are structurally analogous to aortic cusps, but are lighter, thinner, and attached to a muscular rather than a fibrous annulus. In particular, the aortic valves are exposed to large stresses due to the higher blood pressure in the left side of the heart to mediate systemic circulation.

Owing to these hydrodynamic and mechanical factors coupled with heart diseases, aortic valves frequently require repair and/or replacement.

1.1.2 Structure

Heart valves consist of two to three cusps based on the location of the valve. These valvular cusps are complex, highly heterogeneous structures primarily comprised of fibrillar and non-fibrillar extracellular matrix, namely collagen, elastin, and GAGs, which are maintained by interstitial cells. These constituents are systematically arranged and distributed in an anisotropic pattern, forming three distinct cuspal layers: fibrosa, spongiosa, and ventricularis (**Figure 2**). This tri-layered cuspal architecture is adapted to ensuring efficient mechanical and biological durability [2, 14-19].

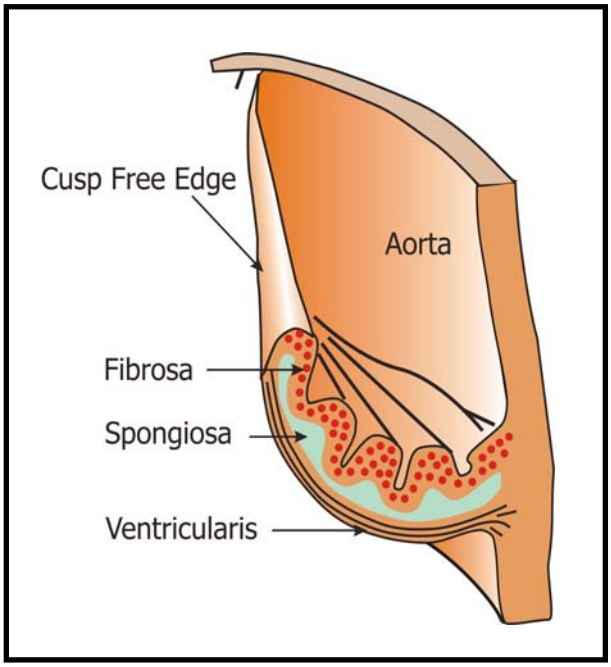

Figure 2: Schematic representation of aortic valve cuspal architecture [20].

The fibrosa, located below the aortic outflow surface of the cusps, is largely responsible for bearing diastolic stresses. This layer is primarily composed of collagen fiber bundles aligned parallel to the free edge of the cusps, providing strength and stiffness to maintain coaptation during diastole. The loading experience by the collagen network is transmitted to the aortic wall by means of the bundles merging at the cuspal commissures [21]. Type I collagen fiber bundles predominate this layer, with significant amounts of Type III collagen, which together account for approximately 43-55% of the total cuspal dry weight [15]. During systole, these circumferentially arranged fibers give rise to corrugations, producing an undulated surface appearance. These microscopic undulations, also known as crimps, create superficial waviness necessary for maintaining coaptation during valve closure as the corrugations disappear to ensure radial compliance (**Figure 3**). Thus, flattening of the corrugations permits elongation of the cuspal tissue with minimal radial mechanical stresses [2, 19]

The ventricularis, a relatively thin layer facing the ventricles, is composed of elastic fibers. These radially directed fibers constitute nearly 11-13% of the total cuspal dry weight [22]. The radial arrangement of the fibers assures tissue extensibility. The elastin sheets impose tensile forces on collagen fibers during valve unloading. Thus, the collagen and elastic fibers are preloaded by virtue of their attachment to each other; the fibrosa under compression and the ventricularis under tension [18]. During diastole, as the collagen fibers realign and extend, the elastic fibers passively extend to accommodate cuspal tissue expansion. The systolic valvular configuration following this cuspal stretch is restored by elastin contraction (**Figure 3**). Thus, elastin sheets in the ventricularis

provide a return-spring mechanism, whereby collagen fibers are restored to their resting geometry via a 'lock-pull' motion to provide maximum coaptation area [17, 20]. The smooth surface maintained by elastin in the ventricularis layer promotes laminar flow during systole [15].

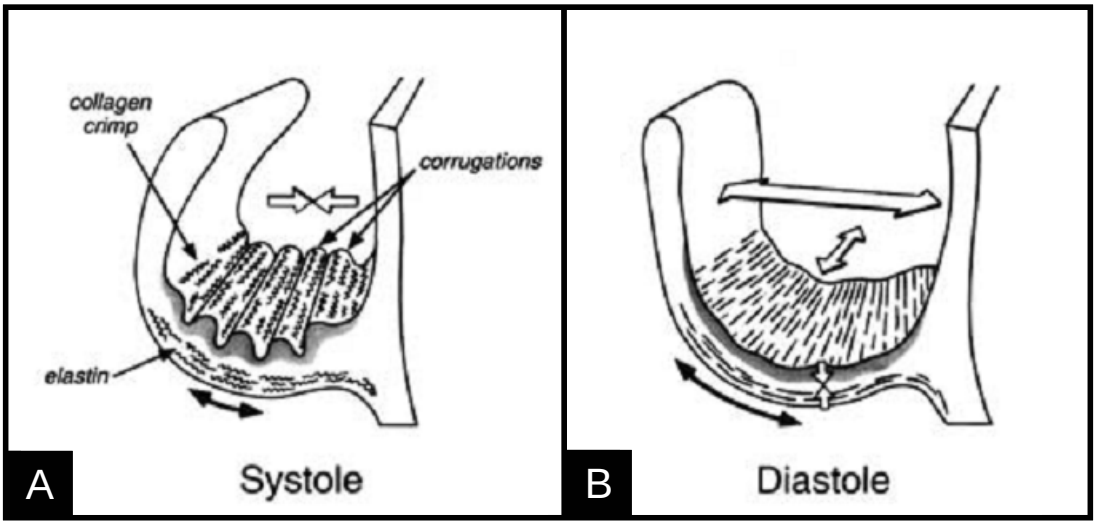

Figure 3: Configuration of collagen and elastin fibers during (A) systolic and (B) diastolic valvular motion [15, 23].

Between the fibrosa and ventricularis lies the spongiosa, which is predominantly composed of non-fibril connective tissue ground substance, specifically glycosaminoglycans (GAGs), and loosely arranged collagen fibers oriented radially. This loose and extremely hydrated amorphous extracellular matrix serves as a 'gel-like' central cuspal layer [2, 4], and thus, conferring plasticity and flexibility to the cuspal tissue [15]. This centrally located layer absorbs compressive loads and cushions shock experienced during valve closing, dissipates shear stresses resulting from oppositional

movement of the two exterior layers during cyclical valve motion, and resists tissue buckling [2, 4, 24, 25].

The fibrosa and ventricularis are surrounded by a single layer of endothelial cells that maintain a non-reactive and thromboresistant blood-contacting surface. These superficially located cells prevent and control plasma and fluid insudation [2, 15, 26]. Another set of functionally important cells include the valvular interstitial cells. These cells play a pivotal role in native valvular tissue by remodeling, replenishing, and synthesizing the local extracellular matrix. Characteristically similar to fibroblast and smooth muscle cells, valvular interstitial cells allow cell-cell communication and confer the valve its ability to contract in response to various chemical factors [15, 26]. Thus, these cellular components regulate and maintain the structural and functional integrity of the valvular tissue.

Therefore, the specialized morphology of the cusps accommodates the dynamic geometric changes during the cardiac cycle by bending, shearing, and buckling to accommodate the functional needs of the heart valve. During repetitive cyclical changes, the non-fibril and fibril structural components of the cuspal tissue reorient and regenerate to respond to the biological and mechanical needs of the valves for proper functioning.

1.2 Glycosaminoglycans

1.2.1 Structure

GAGs are linear acidic polysaccharides containing repeating disaccharide units of uronic acid, either glucuronate or iduronate acid, linked to a modified hexosamine sugar molecular, either N-acetylglucosamine or N-acetylgalactosamine (**Figure 4**).

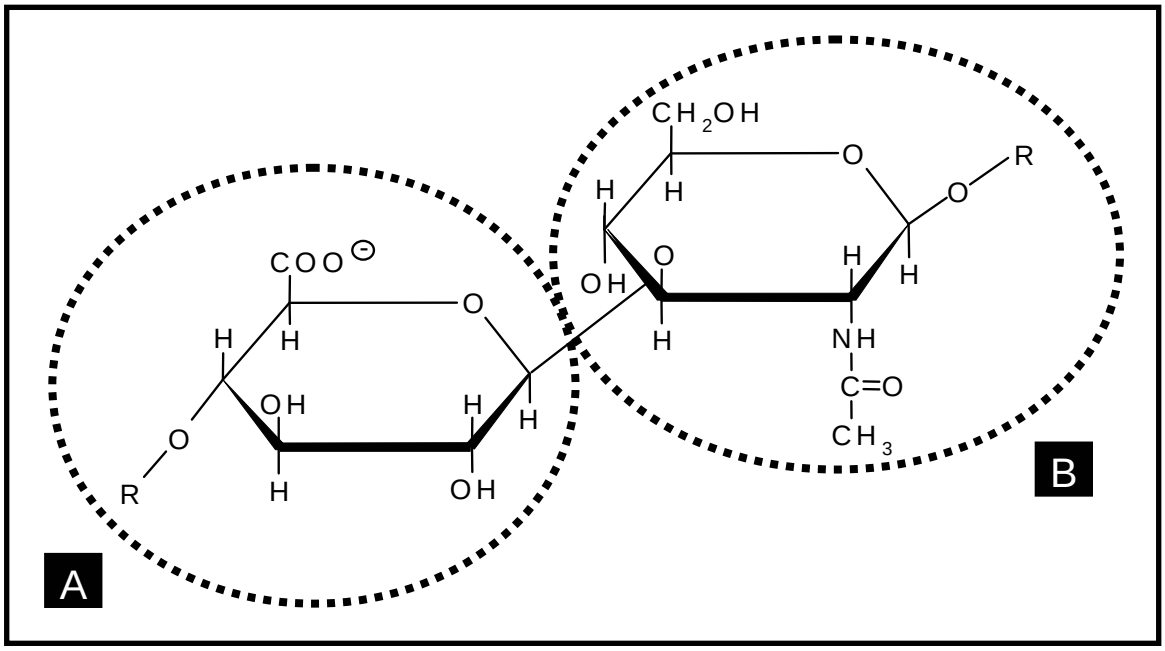

Figure 4: Disaccharide unit of glycosaminoglycan containing (A) uronic acid and (B) hexosamine.

Based on their chemical and structural differences, five species of GAGs exist, namely heparan sulfate/ heparin, chondroitin sulfate, dermatan sulfate, keratan sulfate, and hyaluronic acid. It must be noted that keratan sulfate consists of a galactose in place of the uronic acid. Similarly, the disaccharide composition and geometry of glycosidic linkages varies across the subclasses of GAGs (**Figure 5**). Heparan sulfate consists of

repeating units of D-glucuronic acid and N-acetylglucosamine with 6-N-sulfate group. Chondroitin sulfate and dermatan sulfate comprise of repeating units of N-acetylgalactosamine and D-glucuronic acid with variation in sulfation. Chondroitin sulfate is composed of 4- or 6-O-sulfate group on N-acetylgalactosamine linked to D-glucuronic acid, while dermatan sulfate contains N-acetylgalactosamine with 4-O-sulfate group bond to either D-glucuronic acid or L-iduronic acid. As mentioned previously, keratan sulfate consists of repeating units of galactose (instead of uronic acid) and N-acetylglucosamine with 6-O-sulfate group. Hyaluronic acid, which lacks modification by sulfation, is primarily composed of D-glucuronic acid and N-acetylglucosamine repeat units [27].

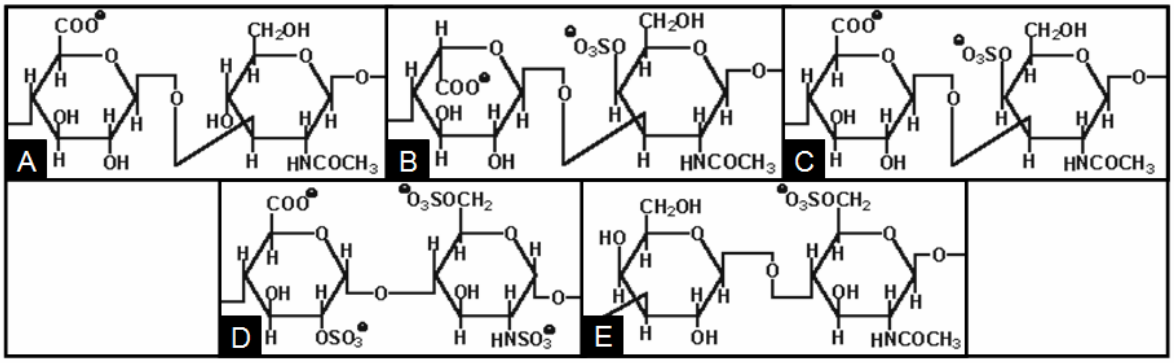

Figure 5: Chemical structures of GAG subclasses: (A) hyaluronic acid, (B) dermatan sulfate, (C) chondroitin sulfate, (D) heparan sulfate, and (E) keratan sulfate.

The carboxylate and sulfated ether of the disaccharide units form a linear array of anionic groups. With the exception of hyaluronic acid, all GAG molecules are attached to a core protein via a glycosidic bond with serine residues. Specifically, a trisaccharide linker segment composed of two galactose residues and a xylose residue is coupled to the

core protein by an O-glycosidic bond to a serine residue in the protein. Some forms of keratan sulfates are linked to the protein core through an N-asparaginyl bond. The presence of multiple serine residues in the core protein allows multiple GAG attachments. The extensions of the chains descending from the core protein produce a bottle-brush appearance of this mucopolysaccharide (**Figure 6**).

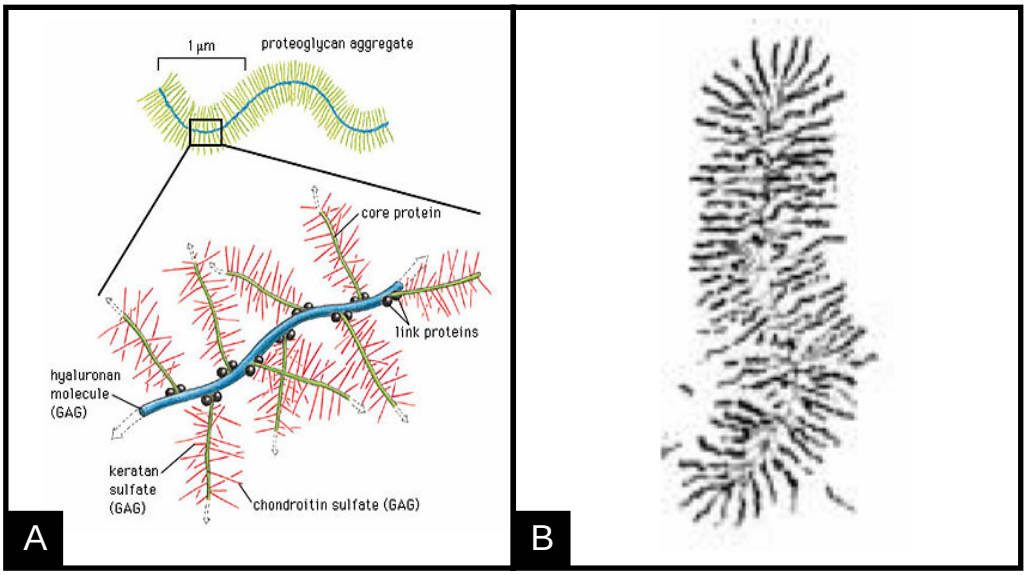

Figure 6: Physical structure of glycosaminoglycan. (A) Four distinct GAG monomers attached to core proteins which are bond to a central strand of hyaluronic acid via link proteins. (B) The extensions of the chains descending from the core protein produce a bottle-brush architecture as seen in this electron micrograph [28].

These GAG chains extend from their polysaccharide backbones due to the presence of negatively charged groups and the relatively higher stiffness of the backbone [29]. Thus, this negatively charged proteoglycan structure forms long, unbranched chains that occupy large hydrodynamic volumes relative to their molecular weights. The negative charges on GAGs give these molecules their water-binding affinity which

allows these macromolecules to assume large domains, and thus, formation of a porous gel matrix. During compression, the intermolecular interactions between adjacent GAGs are decreased as the surrounding solvent displaces. This increases intramolecular interactions between the relatively stiff and polyanionic GAG chains, which subsequently increases the charge density within the maximally compressed domain, causing the macromolecule to propel to its original configuration (**Figure 7**).

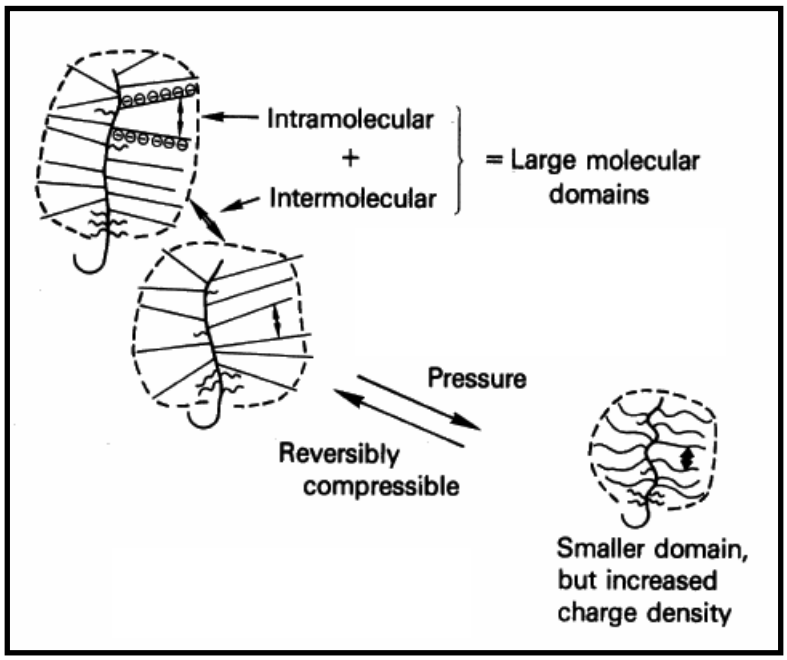

Figure 7: Reversibly compressible property of glycosaminoglycans [29].

1.2.2 Function

GAGs play an important biophysical and biochemical role in maintaining the structural and functional integrity of tissues. These acidic polysaccharides are found in all mammalian tissue and are especially prominent in connective tissue [29].

Biophysically, GAGs posses the ability to reorient and reorganize by binding to water molecules and repelling the negatively charged molecules present on its backbone. Hence, the high viscous behavior and low compressibility typically characteristic of GAG-rich tissues is attributed to the macromolecule's ability to maintain a reversibly compressible hydrated environment [29]. In cartilage, the large quantities of chondroitin sulfate and keratan sulfate found on aggrecan, play an important role in hydration of the tissue [30]. In contrast, the heparan sulfate-rich proteoglycans abundant in kidney glomerular basement membrane aid in filtration of metabolic waste by impeding the passage of anionic serum proteins into the urine [31, 32].

Historically, GAGs were considered inert molecules with the capability to hydrate cells and aid in structural support of the tissue. Recent advances in characterization of the morphology of these extracellular matrix components have led to a greater understanding of the broader biochemical functions of GAGs. In the cellular environment, these macromolecules bind to a variety of proteins and signaling molecules to modulate their activity and consequently influence numerous physiological and pathological processes [33]. In general GAG binding proteins can be categorized in three classes as follows: (a) secreted proteases and anti-proteases, (b) polypeptide growth factors, (c) extracellular matrix proteins and cell-cell adhesion molecules.

Heparin, a modified form of heparan sulfate, has been used as an anticoagulant for several decades. The coagulation cascade is controlled by several serine proteases. A heparin-AT-III ternary complex composed of thrombin and antithrombin III inhibits coagulation proteases (except factor VIIa), thereby preventing coagulation [33]. In the

absence of heparin/heparan sulfate, inactivation of the coagulation cascade by AT-III occurs at a much slower rate.

In addition, heparin sulfate binding with basic fibroblast growth factor (FGF-2) entraps these polypeptide growth factors in the extracellular matrix; thus, enabling GAGs to control the molecular kinematics of the growth factor. Such binding initiates the signaling cascade to facilitate the onset of angiogenesis [33-35]. Similarly, dermatan sulfate binding to FGF-2 and FGF-7 promotes cell growth and wound healing repair. Thus, GAG-binding aids during inflammatory response to injury [27]. Chondroitin sulfate-neural cytokine interactions facilitate neural adhesion, migration, growth patterns as well as inhibiting glial scar tissue formation [36]. Hepatocyte regeneration is modulated by activation of hepatocyte growth factors by dermatan sulfate [37].

GAG binding to extracellular matrix proteins play an important in matrix assembly and organization. Additionally, multi-domain extracellular matrix protein interactions with GAGs mediate cell adhesion to these proteins. GAG macromolecules anchor extracellular matrix components such as collagen fibers to cell-surface receptors. During cellular differentiation and development, GAGs bind to cell-surface receptors to decrease cell-cell adhesion and interactions. By blocking cell-surface receptors, GAGs prevent cell junction formation. Hyaluronic acid binding to CD44 cell surface receptors on cancer cells during metastasis allows diffuse movement of cells and prevents cell-cell adhesion [38, 39]. Similarly, hyaluronic acid-CD44 interactions during myoblast differentiation promote cellular movement [33].

Therefore, it is evident that GAGs influence a myriad of cellular behaviors via its unique morphological attributes.

1.3 Role of Glycosaminoglycans in Heart Valves

The dynamic nature of heart valves during the cardiac cycle continuously subjects the valvular tissue to tensile, compressive, and shear stresses. For this reason, GAGs, a major constituent of the central spongiosa layer of cuspal tissue, play a crucial role in responding to the mechanical and physiological needs of the valve [2, 4, 40]. Combined with their hydrophilic nature, these polyanionic domains maintain a hydrated and viscous environment necessary to sustain the biological and mechanical properties of the tissue.

Of the four heart valves, aortic valvular tissue contains the highest amount of GAGs, comprising approximately 3.5% dry weight of the cuspal tissue [41-43]. As mentioned in the preceding chapters, the aortic valve experiences the highest degree of fatigue due to the high blood pressures resident in the left ventricle to maintain proper systemic circulation. The primary types of GAGs found in aortic cusps include hyaluronic acid, non-sulfated and sulfate chondroitin and dermatan molecules [42]. In human heart valves, hyaluronic acid constitutes the majority of GAGs (60%) found in the tissue; however, an equal ratio of the three GAG subclasses are found in porcine-derived aortic heart valves frequently used for heart valve replacement surgeries [42-45].

In valvular tissue, these mucopolysaccharides exhibit accelerated turnover rates. Interstitial cells present in cuspal tissues synthesize, maintain, and repopulate GAGs in aortic valves. Previous studies show that approximately one-third of the total composition

of hyaluronic acid in the body is replaced daily with the half life of these GAGs ranging from less than one day to several days depending on the tissue [46, 47].

Under physiological conditions, the concentration of GAGs in human aortic heart valve decreases with aging [48]. In heart valves retrieved from patients over the age of 60, a 50% marked reduction in GAG content has been observed [43]. Furthermore, cuspal water content decreases in conjunction with GAG content. Additionally, the onset of calcification is triggered with a decline in GAG content. GAG macromolecules chelate calcium ions, thereby preventing binding with extracellular phosphates in the nucleation of hydroxyapatite crystals [2, 4]. Thus, the presences of GAGs may partly suppress the onset of calcification in heart valves.

By maintaining a hydrated environment necessary for absorbing compressive loads, dissipating shear stresses, and resisting tissue buckling, GAGs preserve the durability of heart valves (**Figure 8**).

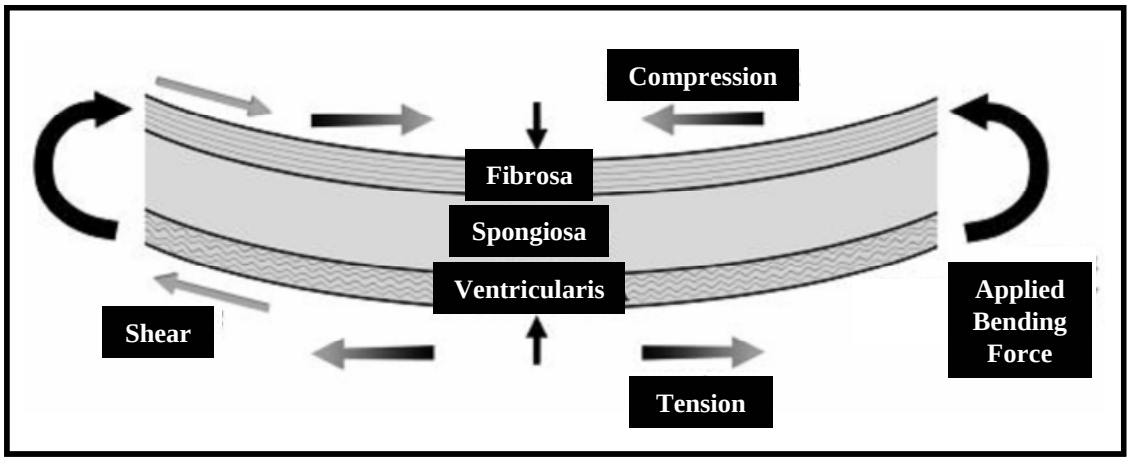

Figure 8: Buffering action of glycosaminoglycans to withstand compressive, tensile, and shear stresses during cyclic loading [49].

These hydrophilic molecules allow the spongiosa to behave like a gel-like layer capable of reversible compression and deformation when subjected to shear forces by the appositional movement of the fibrosa and ventricularis [2, 4, 24, 25]. This buffering action mediated by the presence of water-absorbing GAG molecules, prevents tissue buckling to occur during valvular flexion.

In summation, the valvular cusp's ability to flexibly deform during successive valve cycles, absorb compressive loads during diastolic closing, and dissipate shear stresses experienced during valvular motion are largely possible due to the presence of GAGs in the medial spongiosa layer.

1.4 Heart Valve Diseases and Failure

Valvular heart diseases (VHDs) refer to any condition affecting one or more of the four heart valves that causes subsequent valvular dysfunction. VHD is responsible for nearly 20,000 deaths annually in the United States. The majority of these cases involve disorders of the aortic valve (63%), which bears a heavy burden of regulating systemic circulation, and the mitral valve (14%). Deaths due to pulmonary and tricuspid valve disorders are rarer and account for approximately 0.06% and 0.01% of the cases, respectively [50].

VHD affects normal valvular functioning via (a) stenosis, a reduction of the valvular orifice, which disrupts normal flow of blood through the cusps, and (b) valvular regurgitation or insufficiency that is characterized by backward leak of blood due to inefficient closing of the valves. The primary causes of valvular damage include

improper development of the cusps before birth (congenital) or acquired damage later after birth. Following birth, damage to the valvular cusps can occur by calcific deposition with aging or valvular infection plagued by endocarditis and rheumatic fever [2, 23, 50, 51].

Thus, to remedy this debilitating condition associated with morbidity and mortality, surgical repair or replacement of the damaged and diseased valve must occur since damaged valvular tissue cannot spontaneously regenerate. Valves that cannot be repaired must be replaced by a substitutive heart valve to restore normal blood circulation.

1.5 Characteristics of an Ideal Prosthetic Heart Valve

In order to design a suitable heart valve substitute, the characteristics of such an ideal prosthesis must be defined. In the last 40 years, many valvular replacement options have strived to produce a device capable of accommodating the extensive and elaborate functioning of native valves to ensure adequate, efficient, and effective circulation of the blood.

As initially described by Harken, *et al.*, and modified by several, a quantum leap in the successful design of these prostheses cannot be achieved without addressing the following vital requirements: valvular substitutes must be biocompatible (resistant to infection, nonthrombogenic, and chemically inert); offer little resistance to physiologic flow; capable of prompt and complete closure during appropriate phases of the cardiac cycle; durable; resistant to wear; nonhemolytic and noncalcific; relatively easy to implant

with minimal healing response; noise-free to the patient to prevent discomfort; and must be able to sustain its structural and functional integrity throughout the prosthesis's lifespan, crucial for permanent implantation [2, 52, 53]. However, as discussed in the proceeding sections, many of these goals have yet to be met. Nevertheless, significant strides have been made to achieve fairly safe and efficient models capable of sustaining valvular functional for a short-period of time. Thus, by mastering the above-mentioned characteristics, the durability of these valvular substitutes can be enhanced.

1.6 Current Heart Valve Replacement Options

The rise in valvular failure has led to an increase in the demand for suitable heart valve substitutes. This need for a viable and durable heart valve replacement option has triggered an influx of available prototypes. Development of successful prosthetic heart valves requires biocompatible materials and hemologically tolerant designs. In the past 40 years, numerous models have been designed and investigated for their potential use as ideal heart valve substitutes. Currently, two broad classes of valvular replacement options exist: mechanical heart valves (MHVs) constructed from nonbiological, synthetic materials; and biological heart valves derived from animal tissues [54, 55].

1.6.1 Mechanical Heart Valves

Investigation of the first mechanically fashioned heart valve substitute began nearly 5 decades ago with the successful design and development of the caged-ball

prosthetic Hufnagel heart valve [56]. However, due its limited usage by the population (200 recipients), its validity as a commercially available prosthesis remains disputed.

Presently, approximately 55% of implanted valves worldwide are those designed from non-biological materials [57]. Three primary types of MHVs include caged-ball valves, disc valves, and bileaflet valves (**Figure 9**).

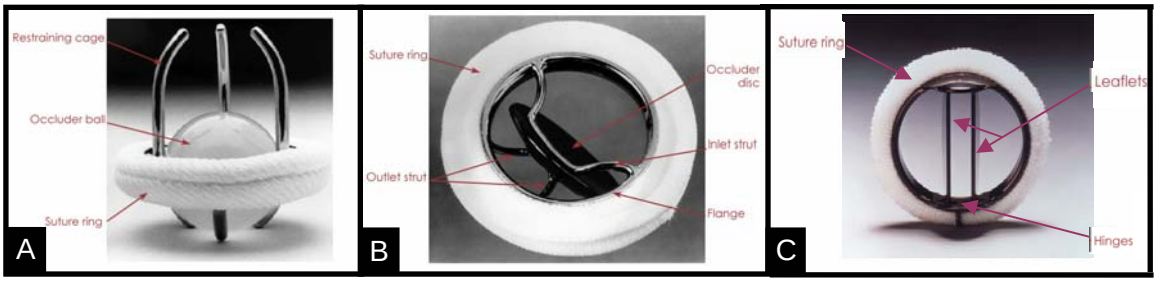

Figure 9: Three primary types of Mechanical Heart Valves: (A) caged-ball; (B) tilting disc; and (C) bileaflet valve [58].

1.6.1.1 Caged-Ball and Non-tilting Disc Valves

Owing to the initial creation of the Hufnagel valve, a methacrylate ball and tube secured with nylon rings, several modified relatively thromboresistant ball valve and non-tilting disc valve designs have been produced as briefly described in **Figure 10**. The non-tilting disc valves included a caged disc configuration with short struts to prevent cocking of the discs. The 1960 design of Starr-Edwards ball valve continues to be used (with modifications) in clinical settings. The modern design includes heat-cured silicon occluder and a cage covered with Teflon fabric [57].

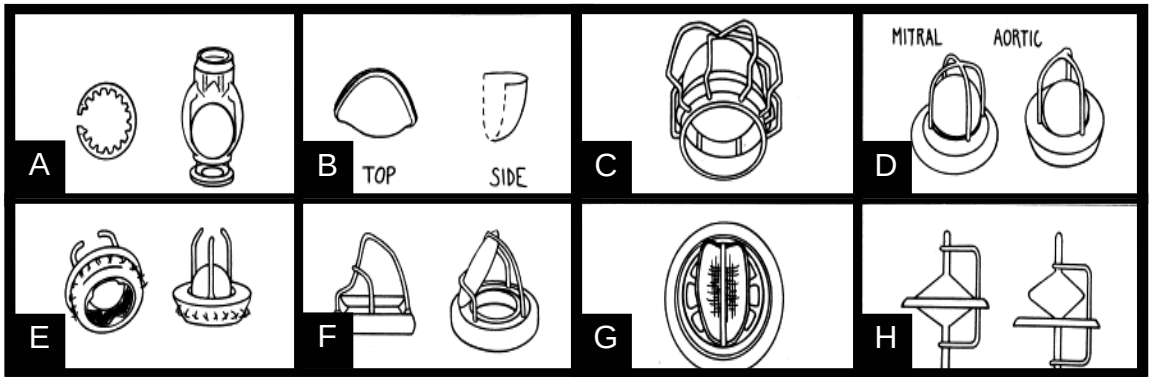

Figure 10: Evolution of ball and non-tilting valves. (A) The original Hufnagel ball valve was developed in 1951; (B) Bahnson fabric aortic cusp valve, a flexible leaflet valve composed of either fabric or silicone-covered fabric; (C) the outer cage of the double caged Harken-Soroff ball valve separated the valves struts from the aortic wall; (D) the 1960 design of Starr-Edwards ball valve continues to be used in clinical settings; (E) The Magovern-Cromie ball valve consisting of curved pins mobilized from the cloth ring of the valve to attach the prosthesis to the native valve annulus; (F) The Lillehei-Cruz-Kaster prosthesis introduced the tilting disc concept to prosthetic valves; (G) The carbon-coated Gott-Daggett prosthesis of 1963 incorporated a silicone-impregnated fabric disc fixed at its diameter to a polycarbonate ring. (H) University of Cape Town-Barnard Aortic valve design included a plunger [56, 57].

1.6.1.2 Tilting Disc Valves

Due to the production of wear particles and potential thromboemboli formation by the ball and non-tilting disc valves, hemodynamically favorable tilting disc valves were introduced. As described in **Figure 11**, the tilting valves evolved over the years, from the Lillehei-Cruz-Kaster (**Figure 10)** tilting disc valve consisting of freely floating disc tilting on the edge of an orifice ring to the production of the Medtronic Hall valve fashioned using a properly oriented carbon coated disc (pyrolytic carbon) retained by titanium struts; currently the most common type of tilting valve in clinical use [56, 57].

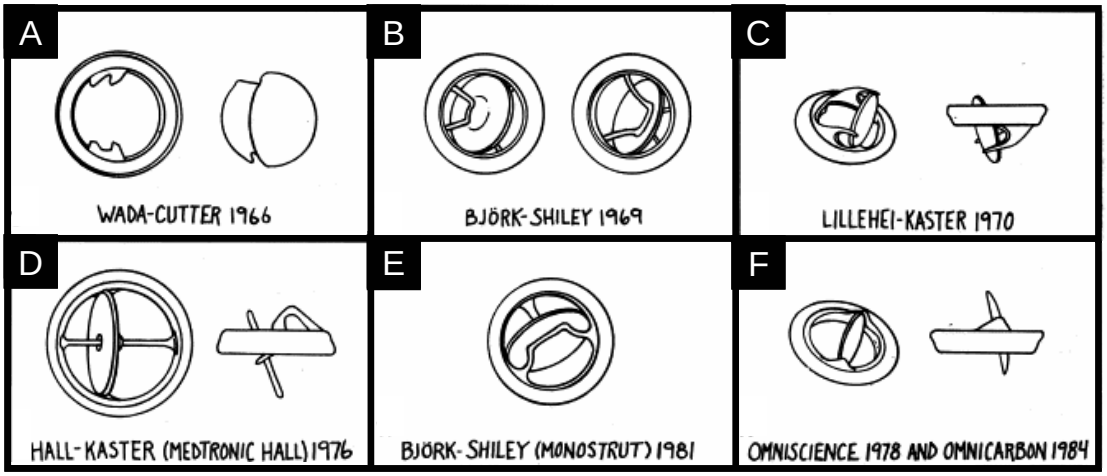

Figure 11: Development of tilting disc valves. Following the birth of the Lillehei-Cruz-Kaster tilting disc valve (*pictured in **Figure 10***), (A) the Wada-Cutter valve was created; (B) the Bjork-Shiley was the first extensively used tilting disc valve; (C) the Lillehei-Kaster valve was constructed using titanium seating and pyrolyte disc; (D) the Hall-Kaster valve was developed by Medtronic; (E) the modified Bjork-Shiley monostrut valve proved better than the originally designed bileaflet valve; (F) this commercially available Omniscience and Omnicarbon valve consists of pyrolyte discs and housing structures [56, 57].

1.6.1.3 Bileaflet Valves

In an effort to improve the thromboresistivity of these valves while retaining the biocompatible nature of the materials, the Gott-Daggett bileaflet valve made its debut in the early 1960's. With improved resistance to clotting, future St. Jude bileaflet prosthesis were introduced in the mid-seventies. These bileaflet valves, which implement the concept of floating hinges located at the central axis of the housing ring, are currently commercially available and widely used for aortic heart valve replacement procedures [56, 57, 59]. Other bileaflet valves currently introduced in the market include Carbomedics valves comprised of a carbon-coated pyrolytic leaflets with a titanium ring, Sorin Bicarbon valves with similar leaflet structures surrounded by a sewing ring, and a

recently released Medtronic Advantage valve model consisting of cylindrical pyrolytic carbon housing with two pyrolytic carbon leaflets housed by a polyester sewing ring [54].

1.6.2 Current State of Mechanical Heart Valves

At present, fabrication of MHVs using biocompatible synthetic materials (**Table 1**) with limited wear resistance, reduced thrombogenic susceptibility, and improved hemodynamic properties has led to the development of successful FDA approved mechanical prostheses (**Table 2**).

Table 1: Biomaterials utilized for Mechanical Heart Valve production [60].

Component	Biomaterials used
Cage, housing or hinge design	Commercially pure titanium or titanium alloys (Ti6Al4V) Cobalt-based alloys (Stellite-21, Haynes-25) Pyrolytic carbon (LTI carbon)
Occluder, disc, leaflet or ball	Pyrolytic carbon (LTI carbon) Silicone rubber Polyacetals (Delrin) Polyolefins (ultra high molecular weight polyethylene)
Sewing ring	Polypropylene Polytetra fluoroethylene (Teflon) Polyethylene terephthalate – PET (Dacron)

Recently FDA approved mechanical valves include the ATS Open Pivot Bileaflet Heart Valve composed of two carbon semilunar leaflets surrounded by a polyester ring, and the On-X Prosthetic Heart Valve designed using carbon-coated graphite-tungsten composite leaflets within a housing surrounded by poly-tetra-fluor-ethylene covered ring [61].

Table 2: FDA approved mechanical prostheses.

Mechanical	Caged Ball	Starr-Edwards
	Tilting Disc	Medtronic Hall Bjork-Shiley Monostrut Omnicarbon Omniscience
	Bi-leaflet	SJM mechanical Carbomedics Edwards MIRA Edwards Suromedics Sorin

The United States MHV market has reached a value of over $360 million, an increase of approximately 3.6% since 2002. This tremendous growth rate is reflective of the technological developments established by the biotechnology industry and the enhancing surgical procedures adopted by the medical community. MHVs hold the largest sector of the United States heart valve market, representing 47.6% of the market; with St. Jude, Edwards Lifesciences, and Medtronic manufactured prosthetic heart valves accounting for up to 90% total of the overall United States heart valve market [62]. St. Jude Medical, the most successful US heart valve company, is the leader in the design and production of MHVs [62].

The steadfast increase in research and development of MHVs has aimed at improving the hemodynamic properties, anticoagulative nature, and the overall durability of these prostheses.

1.6.3 Modes of Failure in Mechanical Heart Valves

The performance of these devices is dependent on the structural design and mechanics of the valve. Numerous retrospective studies have concluded the overall safety of these modern, new generation MHVs. These valves are extremely durable but warrant continual anticoagulant therapy for the duration of the implant, potentially leading to fatal conditions triggered by hemorrhage or stroke. Consequently, such devices are restricted for use by elderly patients with compromised hemodynamic systems and patients suffering from hemolytic conditions.

Despite their high structural integrity, these prostheses are prone to systemic thromboembolism and subsequent, thrombotic occlusion due to flow stagnation occurring at the bileaflet and hinge interface [2, 60]. Biomaterial pitting and degradation, and mechanical erosion of the synthetic materials present potential sites for thrombus formation by exposing corroding and worn areas to thrombotic factors which may eventually cause catastrophic embolism. Likewise, surface erosions can result in occlusion and compromised hemodynamic flow in the valvular construct. Turbulent flow patterns associated with occlusion as well as high flow rates often lead to hemolysis and platelet activation.

The dynamic motion of these MHVs produces a differential pressure gradient that initiates an implosion of vapor filled cavitation bubbles. The formation and collapse of cavitation bubbles compounded with a high pressure jet-stream damages surrounding mechanical structures and native tissue and imposes shear loads on blood particles [60, 63].

Therefore, the primary modes of failure in these prostheses include degradation of the valve components, structural failure, and clinical complications associated with the implanted valve [60].

1.6.4 Biological Heart Valves

Despite recent improvements in the durability and functional efficiency of MHVs, thromboembolic complications due to non-biological surfaces and abnormal flow regimes continue to plaque these structurally stable prostheses. Thus, these aforementioned limitations have led to the development of biological heart valves capable of mimicking many of the physiological properties of native valvular tissue. Biological heart valves include human-derived heart valves; and animal-based bioprosthetic heart valves (BHVs) constructed from either porcine or bovine tissue.

1.6.4.1 Human Tissue Valves

Human tissue valves include cryopreserved cadaveric homografts, autologous valves, and autograft valves which are briefly described in the following sections.

1.6.4.1.1 Cryopreserved Cadaveric Homografts

Aortic and pulmonary heart valves retrieved from human cadavers have been used since the early 1950's [64, 65]. These homografts obtained from healthy cadaveric heart valves retain the natural morphological, physiological, and biomechanical properties necessary for the functional demands of valvular tissue [66]. These grafts contain viable,

living cells that enhance the biocompatibility of valvular leaflets. Despite the relatively low occurrence of thrombotic events, other critical problems continue to restrict the use of these native tissue grafts. The risk of rejection triggered by an immunogenic response can lead to a potentially fatal outcome [67]. Mechanical stresses and injury to the tissue may trigger endothelial activation, which will elicit smooth muscle cell proliferation and cellular apoptosis [68, 69]. Calcification appears to originate in these apoptotic nonviable cells. Additionally, the limited availability of these cryopreserved cadaveric homografts has led to the exploration of suitable substitutes derived from animal cardiac tissues.

Inspired by the above-mentioned valvular replacement option, dura mater cardiac valves, constructed from cadaveric dura mater, made their debut in the 1970s. With glycerol pretreatment, these valves showed low rates of thromboembolism and satisfactory mechanical durability. These valvular constructs, now discouraged because of their susceptibility to transmit communicable diseases, presented another method of using human-tissue to replace dysfunctional valves [70-77].

1.6.4.1.2 Autologous Valves

During a brief period in the 1970s, biological based valves were designed using autologously-derived fascia lata, connective tissue surrounding the patient's mid-thigh musculature, or pericardium harvested from the patients pericardial sac [55]. A tri-leaflet valve was designed to meet immunogenic requirements necessary for a successful valvular implant. Theoretically, these valves pose no immunogenic threat due to their autologous origin. Despite surpassing the host-donor immunological complications, these

autologous valves are technically demanding and do not increase the durability of these bioprostheses [55]. When subjected to physiologically relevant hemodynamic regimes, these valves succumbed to valvular deterioration. The pericardial tissue contracted and formed scar tissue due to the complex bending cycles, turbulent flow, and compressive stresses presented to its interstitial cells [78].

In the face of these failures, other refined designs are currently being pursued. Recently, this approach has been applied to Carpentier-Edwards Perimount pericardial prosthesis that utilizes the patient's pericardium to design the prostheses on a synthetic mounting frame.

1.6.4.1.3 Pulmonary Autografts

In an effort to improve the design of biologically derived valves, the Ross procedure was introduced in the late 1960's. Using pulmonary autografts, the aortic valve is replaced, and a cryopreserved cadaveric homograft is implanted in the pulmonary valvular site [54, 55]. The similarities shared by both semilunar valves and the autologous derivation of the substitute valve permits this clinical procedure to partially overshadow the risk associated with a double valve replacement surgery. In part due to the tedious and complicated surgical procedure, this valvular replacement option is not recommended for older patients. However, with its improved hemodynamics, and the potential for the replacement tissue to become a fully functional dynamic tissue with the ability to remodel, make it an especially attractive valve substitute for younger patients who exhibit low rates of degeneration, thromboembolic events, and endocarditis. Despite

these advantages, one major concern associated with this innovative procedure is the subsequent malfunctioning and failure of these pulmonary homografts which are not natively accustomed to the hydrodynamic and hemodynamic functional demands of the aortic valve [54, 55].

1.6.4.2 Bioprosthetic Heart Valves

The next generation of tissue-based heart valves was introduced to the market to respond to the limited supply of heart valve donors. These xenografts are constructed, partly, from either bovine or porcine tissue (described in greater detail in the subsequent sections).

Furthermore, BHVs may be differentiated by their stented or stentless architectural support (**Figure 12**). Using polymeric stents, stented valves are constructed using xenogenic tissue anchored by three struts and a Dacron ring to secure the cuspal leaflets. The rigid stents utilized for these first generation stented valves caused abrasive cuspal tears and creeping of the struts, resulting in an increased rate of structural deterioration. Advances in material science and engineering have led to the design of improved valves with flexible stents whereby some models utilize biocompatible stent padding to resist tissue abrasion [54, 55, 78, 79].

Figure 12: Stented and stentless Bioprosthetic Heart Valves: (A) stented bovine pericardial valve, (B) stented porcine aortic valve, and (C) stentless porcine aortic valve [80].

More recently stentless valves are increasingly being used for valvular replacement surgeries. These contemporary valves are fashioned using porcine aortic valves dissected with a portion of their subtending aortic wall intact. The absence of a synthetic support structure increases the geometric orifice area necessary for maintaining proper flow. Consequently, the stentless design is credited with retaining as much of the natural hydrodynamic flow pattern characteristic of physiological flow regimes. Whilst the enhanced durability and more physiologic hemodynamic behavior produced by these stentless bioprostheses, the aortic wall is prone to calcification and other structurally-compromising failures. Further research to combat these drawbacks is necessary for identifying ideal bioprosthetic valve architecture [54, 55, 78, 81, 82].

1.6.4.2.1 Bovine Pericardial Heart Valves

These tissue-based valves are fashioned from chemically treated bovine pericardium. Tailored to mimic tri-leaflet or bi-leaflet valves, the design identity of these valvular replacements remains flexible. These valves are chemically treated with glutaraldehyde, a reactive dialdehyde that was shown to preserve the tissue and reduce

tissue antigenicity [83]. The Ionescu-Shiley bovine pericardial valves, introduced in the 1970s, were the first attempt in producing chemically preserved heterografts [79]. However, due to its poor design, these valves deteriorated at a fast pace when implanted. With an improved design, these valves were later modified and manufactured by Edwards Lifesciences. Instead of stitching the tissue to a mounting orifice, the Carpentier-Edwards pericardial valves incorporated a flexible synthetic stent to anchor the pericardial tissue with a modified mounting technique to reduce shear stresses and subsequent tears. Notwithstanding their improved hemodynamic and hydrodynamic properties, as well as hypothetically endless source of supply, the long-term durability of these xenografts remains to be achieved [55, 79]. The variable orientation of collagen fibers in pericardial tissues is not equipped to withstand cyclic loading experienced by native valvular leaflets. Unlike native cusps, pericardial bioprosthesis are incapable of distributing cyclic loads, resulting in high stress concentrations at the commissures of the valves [2].

1.6.4.2.2 Porcine Aortic Heart Valves

The first porcine-derived bioprosthetic aortic heart valve was available in the 1970s; these first generation Carpentier-Edwards and Hancock Medtronic devices were developed using porcine aortic valves secured to a flexible stent to secure the tissue. Like pericardial bioprostheses, these heterografts underwent chemical pretreatment using glutaraldehyde. Owing to their structural and functional similarities to native human aortic valves, porcine aortic bioprosthetic valves maintain nonturbulent,

hemodynamically and hydrodynamically favorable flow regimes necessary to accommodate valvular functional needs. Chemical pretreatment of these bioprosthetic devices at high pressure differentials (80 mmHg) produced visually sound cusps capable of valvular cyclic motion. Nonetheless, these diastolic pressures compromised the extensible nature of the cuspal tissues; thus, making them mechanically vulnerable to buckling at high local curvatures and kinks during bending [2, 79, 84, 85]. Apart from their mediocre biomechanical performance, these valves were prone to calcification.

To combat the propensity of these valves to structural failure, second generation stented and nonstented valves employed glutaraldehyde pretreatment at low to zero pressures. Such nominal pressure differentials prevent distortion of valvular matrix fibers, specifically collagen fibrils. On the contrary, this minimal pressure fixation technique produces smaller diameter valve orifices, necessitating the need for an alternate preparation method. Using a fixation pressure of 40 mmHg at the inlet and outlet of the bioprosthetic assembly, a zero pressure gradient across the cusps is maintained to preserve an appropriate orifice area and cuspal geometry [78]. Current research strategies have focused on coupling conventional chemical tissue fixation methods with antimineralization agents to minimize valvular deterioration and degeneration. These third generation bioprostheses prevent the formation of hydroxyapatite crystals to increase the device's overall durability.

1.6.5 Current State of Tissue-Based Heart Valves

Nearly 300,000 valve replacement surgeries are performed worldwide each year [86]; of which, approximately 45% of these patients receive tissue-based prosthetic heart valves. Bioprosthetic heart valves derived from either bovine or porcine tissue remain the most preferred choice for heart valve replacement surgeries, whereby stented porcine-derived bioprosthetic heart valves, constructed from porcine aortic valves mounted on cloth-covered stents, are the most widely used of these bioprostheses.

Currently, the US BHV industry comprises of a $340 million market with a growth rate of 4.0% [50]. By the turn of this decade, the BHV world market will reach $1 billion [78]. Presently, the BHV market is dominated by valves designed by Baxter-Edwards, Medtronic, and St. Jude [50, 62, 78].

Apart from the FDA approved BHVs (**Table 3**); two commercially available models that continue to dominate the market include Hancock and Carpentier-Edwards bioprosthetic valves. Manufactured by Medtronic, the Hancock valve is constructed using porcine aortic valves pretreated with glutaraldehyde (0.2%) and mounted on Delrin (polyacetal) stents. The Carpentier-Edwards stented BHV is produced by Baxter Cardiovascular. Similar to the previous valve, the Carpentier-Edwards is designed using glutaraldehyde pretreated porcine aortic valves with a metal alloy stent [2].

Table 3: FDA approved bioprostheses.

Bioprosthetic	Stented (Porcine)	Angell - Shiley (AS) xenograft Edwards S.A.V. Medtronic Standard & Mosaic SJM Biocor & Epic
	Stented (Bovine)	Carpentier - Edwards Perimount Ionescu - Shiley Standard
	Stentless	CryoLife O'Brien & SynerGraft Edwards Prima Plus Medtronic Freestyle SJM Toronto SPV & Quattro
	Homografts	CryoLife Homograft

Despite the evolution of BHVs over the past several decades, improving long-term durability must remain the main the objective in order to achieve sizable accomplishments. The durability of these bioprosthesis depends on their ability to resist calcification and mechanical damage. Both processes, either independently and/or synergistically eventuate the ultimate degeneration and deterioration of the valve, prompting re-operation.

Current research aimed at designing BHVs using extracellular matrix stabilizing fixatives coupled with anticalcification treatments is defining a new direction with the potential of achieving the “ideal” replacement valve model. Such strategies will ensure an appropriate longevity of these bioprostheses suitable for long-term implantation without necessitating the need for re-operation.

1.6.6 Modes of failure in Tissue-Based Heart Valves

Unlike their counterparts (MHVs), tissue-derived valves do not require long-term anticoagulation therapy. Due to their inherent biological similarities, these tissue constructs have the ability to support natural and physiologically relevant hemodynamic and hydrodynamic flow regimes. One major drawback of these prostheses is the incidence of structural failure eventuating in valvular stenosis and regurgitation. Triggered by calcific and non-calcific damage, tissue deterioration compromises valvular function. Other complications, addressed in the following sections, include endocarditis and nonstructural dysfunction. Since, porcine-derived bioprostheses are predominantly used for valvular replacement surgeries, the remainder of this chapter will focus on the use of porcine BHVs.

1.7 Porcine Bioprosthetic Heart Valves

1.7.1 Glutaraldehyde Pretreatment of Bioprosthetic Heart Valves

The primary aim of chemical pretreatment of biological tissues is to preserve its structural and functional integrity by inhibiting material degradation, reducing tissue antigenicity, extending shelf-life limit, and maintaining sterility [2].

Currently, glutaraldehyde (1,5-pentanedialdehyde) is the only fixative used to stabilize bioprosthetic heart valves. This commercially available fixative, a reactive dialdehyde, forms stable crosslinks with collagen via a Schiff base reaction of the aldehyde with an amine group of the hydroxylysine/lysine in collagen and by a condensation reaction of two adjacent aldehydes [83, 87]. By stabilizing components of

the valvular extracellular matrix, glutaraldehyde crosslinking partially precludes enzymatic and chemical degradation of the valvular prosthesis. Furthermore, this chemical pretreatment reduces tissue antigenicity and renders it thromboresistive, while imparting antimicrobial sterility [2, 14].

Several shortcomings associated with this aliphatic dialdehyde treatment have triggered the scientific community to seek alternative fixation techniques. Glutaraldehyde crosslinking of bioprosthetic heart valves degrades the endothelial lining surrounding the cusps, which serves to suppress tissue reactivity. Devitalization of interstitial cells prevents the necessary cell-mediated renewal and replacement of extracellular matrix components required to maintain the structural and functional integrity of the tissue. These non-viable cellular regions attract calcium binding and trigger the onset of calcification [2, 88].

Additionally, crosslinking of collagen fibers alters the mechanical property and flexural behavior of the cusps by locking the fibers in a static geometry [89]. During cyclic loading, these crosslinked bioprostheses are incapable of rearranging their fibrous architecture to accommodate tensile, compressive, and shear stresses [18]. This locked state increases tissue stiffness eventuating into abnormal flexural behavior during dynamic valvular motion [90]. Consequently, these glutaraldehyde pretreated bioprosthetic implants are increasingly prone to mechanical fatigue and subsequent valvular failure [4, 18, 19, 24, 25, 84, 85, 90].

Another disadvantage of glutaraldehyde crosslinking is its incomplete stabilization of GAGs, which lack the amine functionalities necessary for aldehyde

fixation. Such inadequacies associated with this chemical pretreatment, diminishes the tissues ability to resist degradation by proteolytic enzymes [3, 4, 8, 9, 40, 42]. GAGs play an important role of maintaining a hydrated environment necessary for absorbing compressive loads, and dissipating shear stresses [4, 24, 25]. Clinical explants indicate a decrease in GAG content, which furthers the implication of GAG loss in valve failure [2, 4, 9]. Furthermore, glutaraldehyde treated cusps buckle to a greater extent during bending than native cuspal tissue [5, 6, 18, 24, 91, 92]. During cyclical bending, GAGs present in the medial spongiosa layer buffer the appositional sliding of the exterior fibrosa and ventricularis layer. Accordingly, depletion of GAGs leads to delamination of the central layer, resulting in structural collapse of the tissue and subsequent valvular degeneration.

Thus, glutaraldehyde pretreatment of BHVs imparts chemical, mechanical, and structural changes that ultimately lead to the demise of the prosthesis. Thus, to increase the durability of these bioprostheses, other fixation chemistries are warranted.

1.7.2 Mechanisms of Failure in Porcine Bioprosthetic Heart Valves

Within a decade of implantation, 20-30% of porcine bioprostheses become dysfunctional and over 50% fail due to degeneration within 12-15 years post-operatively [1, 2, 93]. Despite advances in the design and pretreatment of the valvular prostheses, the durability of these valves is limited. Implant failure can be caused primarily by calcific and/or noncalcific degradation of these bioprostheses.

1.7.2.1 Calcific Degradation

The major cause of implant failure is pathological calcification whereby tissue mineralization occurs. Calcium deposition on the valves causes stenosis, regurgitation, and eventuates cuspal tearing [2, 88, 94-97]. This accumulation of calcium phosphate results in tissue hardening, which ultimately leads to valvular degeneration and failure. This progressive process is perpetuated by host factors, implant-related factors, and mechanical stress related factors [88].

While host factors such as the recipient's age plays an important role in valvular calcification, metabolic rates of calcium, osteocalcin, and vitamin D also mediate its onset [98]. Although, valvular calcification is commonly observed in 10% of the population over 65 years of age, mineral deposition is pronounced in individuals with abnormal levels of the above-mentioned species [2, 69]. Pregnant women also experience a greater degree of calcification due to hormonal changes [2, 69].

Despite the advantageous effects of chemical pretreatment of valvular tissue, glutaraldehyde is one of the most prominent implant factors contributing to dystrophic calcification of the BHVs [2, 88, 98, 99]. While glutaraldehyde pretreatment stabilizes collagen fibers present in valvular tissue, devitalization of interstitial cells occur. These non-viable cells and cellular debris serve as primary nucleation sites to initiate the process of calcification [100, 101]. Due to the cells inability to operate calcium pumps present on its membrane, an influx of freely moving calcium ions into the cellular cytoplasm occurs. These calcium ions bind to the nucleus, lipid-rich membrane, and phosphate-rich intracellular and nuclear components to promote hydroxyapatite

formation. Another synergistic process that contributes to valvular mineralization is the crosslinking of collagen fibers [2, 102]. Glutaraldehyde binds to the amino groups of collagen's lysine/hydroxylysine molecules, resulting in a net accumulation of negatively charged carboxyl groups on the collagen. These exposed carboxyl groups facilitate binding with positively charged calcium ions. Propogation of valvular mineralization further disrupts collagen fibrils which subsequently serve as additional sites for calcium ion deposition. Additionally, loosely bound, unreacted, free aldehydes have shown to further promote calcification by damaging red blood cells at the valvular interface, resulting in cellular necrosis. These cellular fragments promote the onset of calcification [103]. Conversely, implant storage in glutaraldehyde solutions for prolonged durations reduces the tissue's susceptibility to calcification due to decrease in the presence of free aldehydes within the tissue [40, 42].

Intercellularly, GAGs play a role in calcification. Previous studies indicate that the spatial voids within the spongiosa due to loss of GAGs exposes collagen fibers to calcium ion deposition [88, 102]. Thus, by occupying these spaces within the staggered arrangement of collagen fibers, these mucopolysaccharides protect collagen fibers against enzymatic attack and block possible nucleation sites. Additionally, by chelating and sequestering calcium ions to prevent binding with extracellular phosphates, GAGs, particularly hyaluronic acid, inhibit the onset of ectopic calcification [4, 88, 102]. However, other studies dispute the anti-calcific effects of GAGs by elucidating their role as calcification protagonists in cartilaginous tissue [104, 105]. The role of elastin in calcification is poorly characterized. Due to the limited amine functionalities present in

elastin fibers, glutaraldehyde treatment is ineffective in its ability to stabilize and protect these proteins from enzymatic degradation. Deterioration of the protective coating of elastin in BHVs exposes calcium binding sites which subsequently lead to initiation and proliferation of calcium deposition [40, 106].

Mechanical stress incurred by implanted BHVs imposes another venue for calcification [2, 4, 98, 102]. Prior research indicates that calcification is most likely observed in stress concentration regions. These areas exposed to high mechanical stresses and flexural bending during valvular motion results in extracellular matrix disruption, which may potentiate hydroxyapatite formation. The molecular structure of collagen is altered due to fatigue during the cyclical action of the valves [2, 107, 108]. However, it is not clear whether calcium deposition occurs due to disruption of the collagen fibrils or loss of GAGs [4]. It must also be noted that mechanical stress is not a precondition for calcification since calcific deposits are observed in subdermally implanted glutaraldehyde treated valvular tissue [2]. Nonetheless, when compounded with fatigue damage such as abrasion, tearing, and perforations, dysfunction and probable demise of these BHVs is inevitable.

Thus, these host, implant, and mechanical determinants of BHV mineralization contribute to the ultimate failure of BHVs.

1.7.2.2 Noncalcific Degradation

Degradation of valvular structural matrix independent of calcification is another major cause leading to the demise of BHVs. Modes of nonstructural dysfunction includes paravalvular leakage, infective endocarditis, pannus overgrowth, and hemolysis.

The most common cause of nonstructural dysfunction is paravalvular leakage due to poor prosthetic fabrication and/or surgical implantation of the device [109]. Mimicking valvular insufficiency conditions such as regurgitation, paravalvular leakage may be triggered by enzymatic degradation of the annulus supporting the cusps. This condition causes subsequent hemolytic anemia due to irregular flow and penetration of blood cells through the void spaces [110].

The enzymatic degradation of the annulus is often triggered by infective valvular endocarditis. This inflammatory condition is characterized by infection of the endocardium, lining that covers valvular tissue [110]. Often referred to as bacterial endocarditis, infection is instigated by streptococci and staphylococci colonies. These microorganisms can distort the structural integrity of the valves by piercing through its walls and consequently, disrupting normal valvular functioning. Clusters of infection can stimulate formation of emboli. Thus, bacterial infection can lead to valvular morbidity and consequently, mortality of the patient [94, 109, 111-113].

Valvular failure by pannus overgrowth is caused by the interference of normal valve operation by an excessive healing response at the interface of the sewing ring and the host tissue. Triggered by an immunogenic reaction, macrophages and giant cells are recruited to the site [114]. With its ability to stimulate fibroblast growth, macrophages

elicit fibrous tissue formation. This overgrowth reduces the available orifice area, leading to stenosis of the valve which impedes normal blood flow. Tears may also occur at the site of healing. Thus, such foreign body reaction may lead to the dysfunction of the valve [115].

Valvular degeneration associated with damaged, calcified, and torn cusps produce turbulent flow around the valve opening. Such violent and unstable flow patterns around the dynamic valvular tissues causes severe hemolysis due to shearing of the blood cells. More prevalent in MHVs, hemolysis in BHVs occurs at sub-clinical levels [116]. If undetected and untreated, such blood damage can eventually lead to fatal anemic conditions and thromboemboli formation at the distorted tissue region [94].

Another catalyst for valvular degeneration, mechanical stress, damages the structural matrix of BHVs; thus, compromising the functional anatomy of valves [5, 6, 18, 19, 24, 25, 90, 91, 94, 107]. Noncalcific structural damage of the valves can accrue at stress concentration regions during cycling motion of the valves. As a result stress accumulation can lead to cuspal fatigue and tearing [2].

Glutaraldehyde pretreatment inhibits the dynamic structural rearrangements to accommodate natural valve functioning [89]. This alteration in the valves ability to remodel its extracellular matrix components results in increased flexural stress due to abnormal flexion [90, 117, 118]. During the cardiac cycle, these valves are continuously subjected to tensile, compressive, and shear stresses. Cyclic fatigue of these BHVs imposes many structurally deteriorating problems such as decrease in flexural stiffness and tensile strength of the valves; thus, making the cusps vulnerable to material failure

[19, 25]. Loss of cell-mediated remodeling and replenishment of the extracellular matrix predisposes theses valves to extensive valvular damage. Thus, these BHVs clinically fail due to degeneration during cyclical loading and unloading of valvular tissue.

Another mechanism of valvular deterioration is the interlayer shearing and compressive tissue buckling of the valve [5, 6, 24, 25, 92, 94]. Loss of GAGs along with tissue stiffness imparted by glutaraldehyde fixation contributes to abnormal flexural patterns during valvular motion. The central layer, spongiosa, rich in GAGs mediates the differential movement of the two external layers by absorbing compressive and tensile loads. During valvular bending, cusps fixed with glutaraldehyde buckled to a greater extent than native valvular cusps [5, 6]. Tissue buckling can be attributed to the loss of GAGs and to the cuspal tissues diminished ability to hydrate its central layer to dissipate shear stresses [24, 25, 119]. Hence, inability of the cusps to accommodate the dynamic motion of the tissue during diastole and systole can result in delamination, fracture, and loss of collagen fibers. Therefore, mechanically mediated valvular deterioration can lead to the subsequent failure of BHVs.

1.7.3 Valvular Tissue Buckling

Tissue buckling is defined as tissue deformation whereby the length and compressive stresses are reduced in exchange for local structural collapse. Buckling occurs at areas of sharp bending where large stresses accumulate [5].

Previous studies have concluded the effect of collagen fiber disruption on compressive tissue buckling characteristics of BHVs. Systemic disruption in collagen fiber morphology induces compressive buckling at that site when subjected to high bending curvatures. Furthermore, it has been shown that glutaraldehyde crosslinked cuspal tissue buckled to a greater extent than untreated cusps when subjected to such sharp bending configurations. This difference in buckling patterns is largely attributed to the potential change in shear properties of the valvular tissues. Unable to distribute and reduce the internal stresses subjected during such bending, these cusps experience compressive buckling characterized by crinkling of the tissue [5, 6].

During diastolic valvular motion, the cusps are subjected to compressive loads. The spongiosa, which is rich in GAGs, is responsible for the absorption of compressive loads. One of the major disadvantages of glutaraldehyde pretreatment is its inability to stabilize GAGs [3, 4, 7, 10]. These hydrophilic molecules permit cushioning of the compressive, tensile, and shear stresses experience by valves during the repetitive cardiac cycles [2, 4, 24, 25]. Thus, unable to absorb the compressive loads presented during bending due to alterations of the natural-strain reducing configuration assumed by normal functional valves, these bioprostheses produce kinks and sharp bends during flexion, resulting in tissue buckling [6]. Tissue buckling sites serve as focal points of tissue stress [18, 19, 120]. Cyclic valvular motion accompanied by tissue buckling can lead to eventual fatigue and tearing of the valves. Thus, stabilization of GAGs using GAG-target fixation chemistries may preclude the extent of tissue buckling in BHV, and subsequently, improve the durability of these bioprostheses.

CHAPTER 2

CURRENT RESEARCH RATIONALE

2.1 Overview

In spite of the advent of numerous available porcine-derived BHV models, the ideal bioprosthetic implant remains to be achieved. Current bioprosthetic prototypes are plagued with structural and non-structural dysfunctions. To extent the durability of these bioprostheses, the structural and functional attributes of these tissue-based valves must be maintained.

Currently, BHVs are pretreated with glutaraldehyde, a commercially available fixative. Glutaraldehyde is credited with crosslinking the collagenous component of these bioprostheses. However, such pretreatment does not stabilize valvular GAGs. These extracellular matrix components, predominantly present in the medial spongiosa layer of cusps, play an important role in regulating physico-mechanical behavior of the cuspal tissue during dynamic motion. Another deficiency of glutaraldehyde fixation is the altered flexural behavior of the cusps, ensuing in buckling of the cuspal tissue. Propagation of such tissue deformations subsequently leads to the ultimate failure of these bioprostheses. Thus, to sustain the dynamic nature of these valves, it is important to stabilize cuspal GAGs. Accordingly, the primary objective of this study is to reduce valvular tissue buckling in BHVs by stabilizing cuspal GAGs using GAG-targeted fixation chemistries.

2.2 Specific Research Aims

Aim I: To Examine the Role of Glycosaminoglycans in Valvular Tissue Buckling?

Hypothesis: Glutaraldehyde crosslinked cuspal tissue may buckle to a greater extent than fresh, untreated cusps. Following enzymatic digestion of GAGs, these tissues may experience a marked increase in buckling pattern, suggesting that the loss of GAGs may play a role in valvular tissue buckling.

Experimental Plan: Buckling behavior will be assessed by quantifying the extent of buckling in the two aforementioned cuspal groups prior to and following exposure to GAG-degrading enzymes. Additionally, surface buckling outlines of the cusps will be characterized by determining the change in the number of buckles with increasing curvatures. Also, bending configurations will be qualitatively examined via histology. These results will be supplemented with quantitative GAG content and cuspal hydration analyses.

Aim II: To Determine if Stabilization of Glycosaminoglycans Reduces Tissue Buckling in Bioprosthetic Heart Valves?

Hypothesis: The retention of valvular GAGs may reduce the extent of buckling. Valvular tissue treated with GAG-targeted fixation chemistries may experience a lesser degree of buckling than glutaraldehyde pretreated cusps. Moreover, neomycin trisulfate bound cuspal tissues may exhibit the least amount of buckling following enzymatic degradation of GAGs compared to other chemically fixed tissues, mimicking fresh tissue buckling pattern.

Experimental Plan: To assess the efficacy of GAG-stabilizing fixation, the buckling behavior of each cuspal treatment will be evaluated. As mentioned above, the buckling depth will be evaluated before and after GAG-digestive treatment. Furthermore, surface buckling outline of the bent cusps will be characterized using the previously stated qualitative and quantitative analyses as well as using scanning electron microscopy. In addition, quantitative GAG content and cuspal hydration analyses will be conducted.

Aim III: To Investigate if Stabilization of Valvular Glycosaminoglycans Using Neomycin Trisulfate - Enhanced Glycosaminoglycan - Targeted Fixation Chemistry Precludes Tissue Buckling in Fatigued Bioprosthetic Heart Valves?

Hypothesis: Ongoing studies indicate that cusps with bound neomycin trisulfate resist GAG depletion during *in vitro* cyclical fatigue than those cuspal tissues pretreated with glutaraldehyde. Stabilization of GAGs using neomycin trisulfate will improve valvular durability by resisting tissue buckling after fatigue cycling. Thus, the buckling pattern in the abovementioned cuspal fixation groups may remain the same as previously seen, but the extent of buckling may be pronounced due to cyclical fatigue.

Experimental Plan: To ascertain the effect of cyclical fatigue and valvular GAG retention on cuspal tissue deformation, valvular tissue buckling behavior following *in vitro* cyclical fatigue will be assessed using the previously mentioned qualitative and quantitative methods. Buckling patterns of statically stored cusps will be evaluated as controls.

CHAPTER 3

MATERIALS AND METHODS

3.1 Materials

Porcine aortic heart valves were obtained from a local USDA approved abattoir, Snow Creek Meat Processing, Seneca, SC. The following materials were purchased from the noted vendors and used in the present studies: ammonium acetate, neomycin trisulfate salt hydrate, glutaraldehyde (50% stock), hyaluronidase (from bovine testes, type IV-s, 3,000–15,000 U/mg), chondroitinase ABC (from *Proteus vulgaris*, lyophilized powder, 50–250 Umg), D(+)-glucosamine-HCL, collagenase Type VII from *Clostridium histolyticum*, 1-9- dimethylmethylene blue (DMMB) were all purchased from Sigma-Aldrich Corporation (St. Louis, MO); 1-ethyl-3-(3-dimethylaminopropyl) carbodiimide (EDC), n-hydroxysuccinimide (NHS) from Pierce Biotech (Rockford, IL); *p*-dimethyl aminobenzaldehyde, acetyl acetone, and 4-(2-hydroxyethyl)-1-piperazineethanesulfonic acid (HEPES) were purchased from Fisher Scientific (Fair Lawn, NJ); and 4-morpholinoethanesulfonic acid hydrate (MES) hydrate was obtained from Acros Organics, NJ

3.2 Methods

3.2.1 Tissue Harvesting and Fixation

Fresh porcine aortic heart valves were obtained from a local abattoir and thoroughly rinsed in ice-cold saline. Within 3-hours of harvesting, intact aortic valves were stuffed with cotton to maintain diastolic morphology and chemically crosslinked in three fixation groups as follows:

Group I: 0.6% Glutaraldehyde in 50 mM 4-(2-hydroxyethyl)-1-piperazineethanesulfonic acid (HEPES) buffered saline solution at pH 7.4 at ambient temperature for 24 hours followed by 0.2% Glutaraldehyde in 50 mM HEPES buffered saline solution at pH 7.4 for 6 days at ambient temperature.

Group II: 30 mM EDC / 6 mM NHS solution buffered with 50 mM 4-morpholinoethanesulfonic acid hydrate (MES) at a pH of 5.5 for 24 hours at ambient temperature. Following the carbodiimide fixation, valves were thoroughly rinsed in a 50 mM HEPES buffered (pH 7.4) saline solution and subsequently crosslinked with 0.6% glutaraldehyde for 24 hours followed by storage in 0.2% glutaraldehyde for the remaining 5 days.

Group III: 1 hour incubation in 1 mM neomycin trisulfate solution comprised of MES buffer solution at a pH of 7.4. Next, valves were thoroughly rinsed with deionized water and subsequently fixed with carbodiimide fixation chemistry as outlined above, followed by storage in 0.2% glutaraldehyde.

Group IV: Fresh porcine aortic valves that were not chemically fixed were used as controls to observe buckling in native valve tissue.

3.2.2 Enzymatic Degradation of Glycosaminoglycans

Following the above-mentioned respective tissue fixation and storage procedures, cusps were excised from their subtending aortic walls and thoroughly rinsed in 100 mM ammonium acetate buffer (pH 7.4). Whole cusps were incubated in 1.2 ml of 10 U/ml high purity hyaluronidase and 0.2 U/ml high purity chondroitinase ABC buffered in the aforementioned ammonium acetate buffer for 24 hours at 37^{o}C under vigorous shaking at 650 RPM. Fresh cuspal tissue exposed to these enzymatic conditions have shown to completely deplete the valvular tissues of GAGs [3]. Following incubation in enzyme-buffered solutions, samples were thoroughly rinsed in deionized water.

3.2.3 *In Vitro* Cyclic Fatigue

Following the above-mentioned respective tissue fixation and storage procedures (**3.2.1 Tissue Harvesting and Fixation)**, valves were mounted on Delrin stents for accelerated wear testing. Using a Dynatek M6 machine (**Figure 13**), 3 stented valves from Group I and Group III were tested at 700 cycles/minute and subjected to 10 million cycles in the accelerated fatigue tester, equivalent to 3-4 months of normal adult cardiac cycle. Daily tests included stroboscopic observations and pressure checks. After fatigue testing, the retrieved valves were photographed and analyzed for macroscopic signs of wear, abrasions, and tears. Cusps were dissected from their insertion in the aortic wall and the extent of buckling depth was evaluated (procedure described in the proceeding sections).

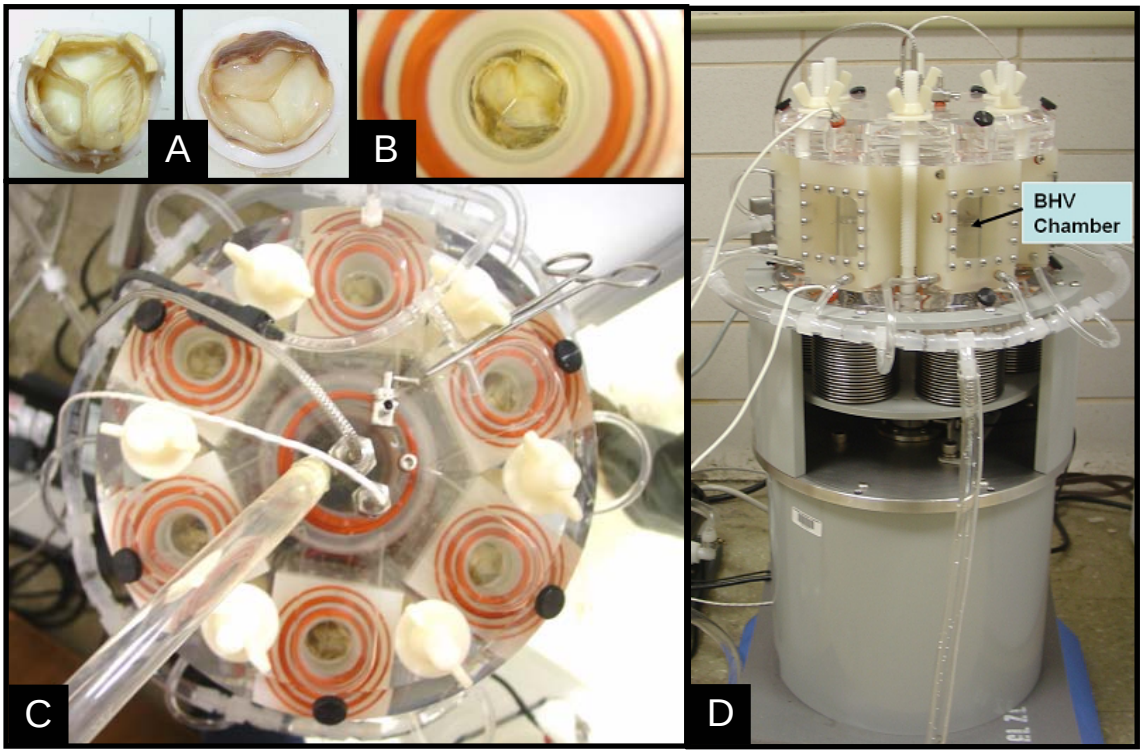

Figure 13: *In vitro* cyclic fatigue testing. (A) Stented porcine heart valves; (B) stented porcine heart valves placed in fatigue tester chamber; (C) a set of 6 stented porcine heart valves undergoing accelerated fatigue testing; (D) Dynatek M6 machine.

3.2.4 Specimen Bending Preparation

Following the above-mentioned preparations, cusps were excised from the aortic root and circumferential strips were obtained from the belly region of the cuspal tissue. These 5 mm wide strips were bent to desired curvatures by bending them against natural curvature to mimic physiological bending in the belly region of cusps (**Figure 14**).

During valvular motion, irregular folding of bioprosthetic cusps occurs. Due to inextensible nature of bioprosthetic heart valves, reverse bending curvatures, characterized by the fibrosa on the outside of the bend, are observed in the belly region of cuspal tissue in diastole [5, 121].

To maintain a bent configuration of the cusps, stainless steel pins were pierced through either ends of the strips; the ends were separated to a desired radius of curvature; and held in place by using cork stoppers at either ends of the pin for 24 hours in 0.2 % Glut solution.

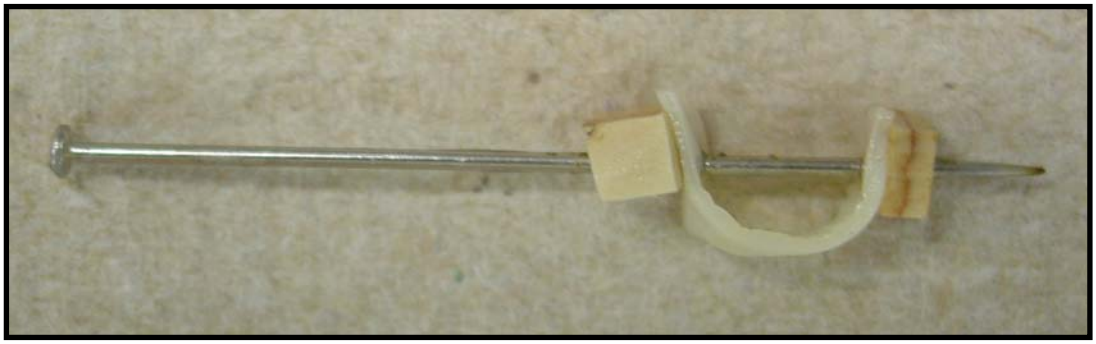

Figure 14: Circumferential cuspal strips bent against natural curvature. To maintain a bent configuration, stainless steel pins were pierced through either ends of the strips; the ends were separated to a desired radius of curvature; and held in place by using cork stoppers at either ends of the pin.

The radius of curvature was varied by changing the length of the tissue to satisfy the following relationship:

$$s = r \bullet \theta_{radians}$$

whereby s denotes the arc length of the curvature, r represents the desired radius of curvature, and $\theta_{radians}$ is the radian angle of the arc. In this case, a radian angle of π was used to represent a semi-circular arc produced by the bent cuspal strips.

3.2.5 Histological Preparation

Routine histological preparations of the paraffin-embedded samples were performed to quantify the extent of buckling. To visualize and identify GAGs, Alcian blue staining with Brazilliant!® nuclear fast red (Anatech Ltd., Battle Creek, MI) counterstain was used. Briefly, 5 μm thick paraffin sections were deparaffinized and hydrated with distilled water, mordant in 3% aqueous acetic acid for 3 minutes, followed by staining with 1% Alcian Blue in 3% acetic acid at pH 2.5 for 30 minutes. After thorough rinsing, sections were counterstained with the above-mentioned nuclear fast red stain (0.1%) for 5 minutes, thoroughly rinsed, and dehydrated for subsequent mounting and coverslipping.

3.2.6 Tissue Buckling Quantification

Following histological evaluation of the samples, the extent of buckling was quantified using a Zeiss Axioskop 2 plus (Carl Zeiss MicroImaging, Inc., Thornwood, NY) in conjunction with SPOT Advanced software. Using measuring and drafting functions such as circular and linear dimension line features of the SPOT Advanced software, the actual curvature of the bending, tissue thickness, and depth of buckling were measured. To determine the radius of curvature, a circle was fitted visually to the semi-circular arc of the tissue. The tissue thickness was measured by averaging the local thickness of the tissue away from the sites of tissue buckling. Depth of tissue buckling was quantified by measuring the distance between the deepest point of buckling and the

inner boundary of the tissue thickness (**Figure 15**). The fractional depth of buckling represents the ratio of buckling depth to the local tissue thickness.

To normalize the variation in tissue thickness between samples, the curvature was multiplied by the local thickness of tissue. Thus, both variables, curvatures and tissue thickness, affect the degree of buckling depth.

Per histological observations, it was evident that as the radius of curvature decreased or as the curvature of bending increased, the extent of buckling increased. To demonstrate this relationship, fractional depth of buckling versus the product of tissue thickness and curvature of bending were plotted as described previously by Vesely, I. *et al* [5, 6]).

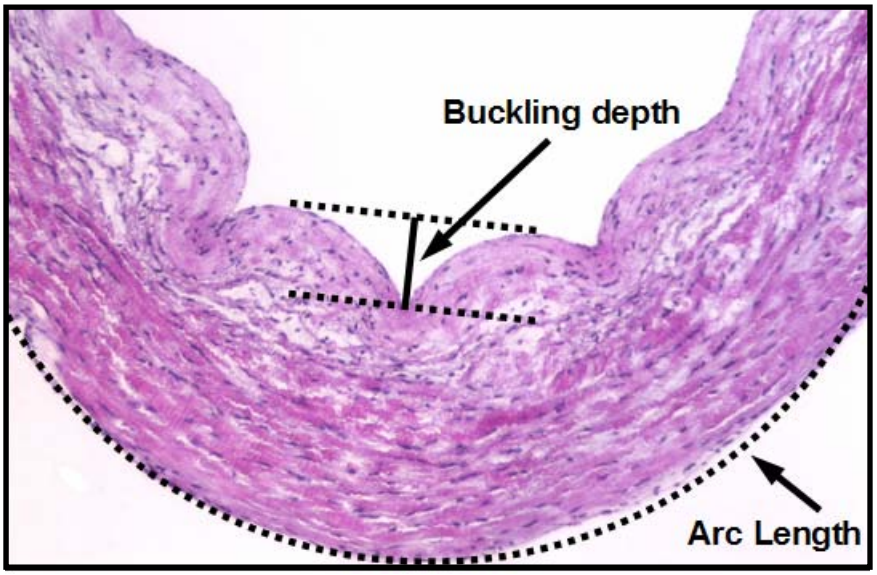

Figure 15: Tissue buckling quantification. Depth of tissue buckling was quantified by measuring the distance between the deepest point of buckling and the inner boundary of the tissue thickness. Arc length was determined by fitting a circular function around the bending arc of the tissue.

Additionally, to assess the affect of chemical fixation on the surface buckling outline produced by valvular tissue bending, the number of buckles present in the semi-circular arc of bent cuspal strips was calculated. This data was plotted against the product of thickness and curvature to observe the change in the surface buckling outline of cusps when subjected to various bending configurations.

3.2.7 Qualitative Assessment of Tissue Buckling using Scanning Electron Microscopy

Following the above-mentioned respective tissue fixation and storage procedures, and specimen bending preparations, lyophilized samples were mounted on aluminum alloy stubs. An ultra-thin coating of gold-palladium was applied using Denton Vacuum Desk II sputter coater. A low vacuum, high resolution environmental scanning electron microscope (JSM 5300 LV ESEM; Joel Ltd, Tokyo, Japan) was used at 5.0 kV to capture images at various magnifications ranging from 35 to 100 X.

3.2.8 Glycosaminoglycan Quantification by Hexosamine Analysis

Previously published methods were employed to quantify total hexosamine content in the respective tissue groups [3]. Briefly, lyophilized cusps were acid hydrolyzed using 2M hydrochloric acid for 20 hours at 95°C in a vacuum desiccator. After thorough drying under nitrogen gas flow in a boiling water bath, tissue hydrolysates were dissolved in 2 ml of 1M sodium chloride solution and reacted with 2 ml of 3% acetyl acetone in 1.25M sodium carbonate. Next, theses samples were incubated for 1 hour at 96°C. Following thermal equilibrium at room temperature, samples were treated

with 4 ml of absolute ethanol with subsequent addition of 2 ml of Ehrlich's reagent (0.18 M *p*-dimethylaminobenzaldehyde in 50% ethanol containing 3 N HCl). An incubation period of 45 minutes at room temperature allowed formation of a color product reflective of the hexosamine quantities present in the cuspal tissue. Using the optical absorbance readings of the tissue hydrolysate and D(+)-glucosamine (0 – 200 μg) standards at 540 nm, the hexosamine quantities were determined.

3.2.9 Glycosaminoglycan Quantification by Dimethylmethylene Blue Assay

Following fixation and enzymatic digestion of GAGs using above-mentioned procedures, GAGs released into the enzyme solutions (10 U/ml high purity hyaluronidase and 0.2 U/ml high purity chondroitinase ABC buffered in 100 mM ammonium acetate buffer at pH 7.4) were quantified by 1-9- dimethylmethylene blue (DMMB) assay using previously described methods [10, 122-124] with minor modification as described below. In a 96 well-plate, 20 μl of the aforementioned enzyme solution, 30 μl of PBE buffer solution (100 mM Na_2HPO_4, 5 mM EDTA, pH 7.5) and 200 μl of DMMB reagent solution (40 mM NaCl, 40 mM Glycine, 46 μM DMMB, pH 3.0) were added to each well. Next, optical absorbance readings were read at 525 nm. Serving as controls, optical absorbance readings of GAG release in buffer solution (100 mM ammonium acetate buffer at pH 7.4) using the aforesaid buffer with PBE buffer solution and DMMB reagent solution were obtained. To observe GAG loss in GAG-digestive enzyme solution, chondroitin sulfate (0 – 1.25 μg) standards treated with 20 μl of the above-mentioned enzyme solution were used. Likewise, chondroitin sulfate (0 – 1.25 μg) standards without

any exposure to GAG-degrading enzymes were employed to determine GAG release in buffer solution.

3.2.10 Initial Water Content and Rehydration Capacity of Fixed Cuspal Tissue

Whole cusps were either incubated in 100 mM ammonium acetate buffer at pH 7.4 or incubated in 1.2 ml of 10 U/ml high purity hyaluronidase and 0.2 U/ml high purity chondroitinase ABC buffered in the aforementioned ammonium acetate buffer for 24 hours at 37^{o}C under vigorous shaking at 650 RPM. Following incubation with GAG-degrading enzymes or buffered solution, cusps were thoroughly rinsed with deionized water. Using three stacked tissue papers folded in half (Kimwipes EX-L Delicate Task Wipers, Kimberly Clark Inc., Roswell, GA), excess water on the periphery of the cusps was carefully removed without applying pressure; instead gently dabbing the valvular tissue. The wet weight of each cusp was recorded prior to lyophilization. Following a lyophilization period of 24 hours, the cuspal dry weights were recorded. Initial Water content was then calculated as follows:

$$Water\ Content\ = \frac{Wet\ Tissue\ Weight - Dry\ Tissue\ Weight}{Wet\ Tissue\ Weight}$$

The rehydration capacity of fixed cuspal tissue was determined by rehydrating the tissue samples in 1.5ml of deionized water for 24 hours at 4^{o}C. The wet weight was determined and the rehydration capacity was calculated as follows:

$$\mathrm{Re}\,hydration\;\;Capacity\;=\;\frac{\mathrm{Re}\,hydrated\;\;Tissue\;Weight-Dry\;\;Tissue\;Weight}{Dry\;\;Tissue\;Weight}$$

3.2.11 Statistical Analyses

Results obtained by hexosamine analysis and water content and rehydration studies are expressed as a mean ± the standard error of the mean (SEM). Statistical analyses for these results were performed using single-factor analysis of variance (ANOVA) whereby significance was defined as $p < 0.05$.

Graphical analysis of valvular tissue buckling behavior was conducted by fitting a linear regression to the data set. Statistical comparisons of the trendlines were performed using two-sample t-test of the predicted values obtained from the regression. Two near-boundary curvatures representing high and low bending radii were selected to evaluate cuspal buckling patterns. Significant differences were defined as $p < 0.05$.

CHAPTER 4

RESULTS

4.1 The Role of Gycosaminoglycans in Valvular Tissue Buckling

To examine the potential role of GAGs in valvular tissue buckling, glutaraldehyde crosslinked and fresh, untreated cusps were subjected to varying radii of curvatures. Additionally, to observe buckling in GAG-depleted valvular tissue, these cusps were exposed to GAG-digestive enzymes prior to evaluation of tissue buckling pattern when subjected to different bending curvatures.

Histologically, it was evident that the extent of buckling increased with decreasing radii of bending or with an increase in curvature (**Figures 16 and 17**). Of note, a greater depth of buckling in general was observed in cusps pretreated with glutaraldehyde compared to fresh, untreated cusps. With exposure to GAG-degrading enzymes, glutaraldehyde pretreated cusps experienced an additional increase in buckling depth.

Furthermore, histological staining for the presence of GAGs indicated a depletion of GAGs in GAG-digested tissues (**Figures 16 and 17: D, E, F**). A dramatic decrease in GAG staining was observed in GAG specific staining of glutaraldehyde crosslinked cusps treated with GAG-digestive enzymes, indicating a loss of GAGs (**Figure 17**).

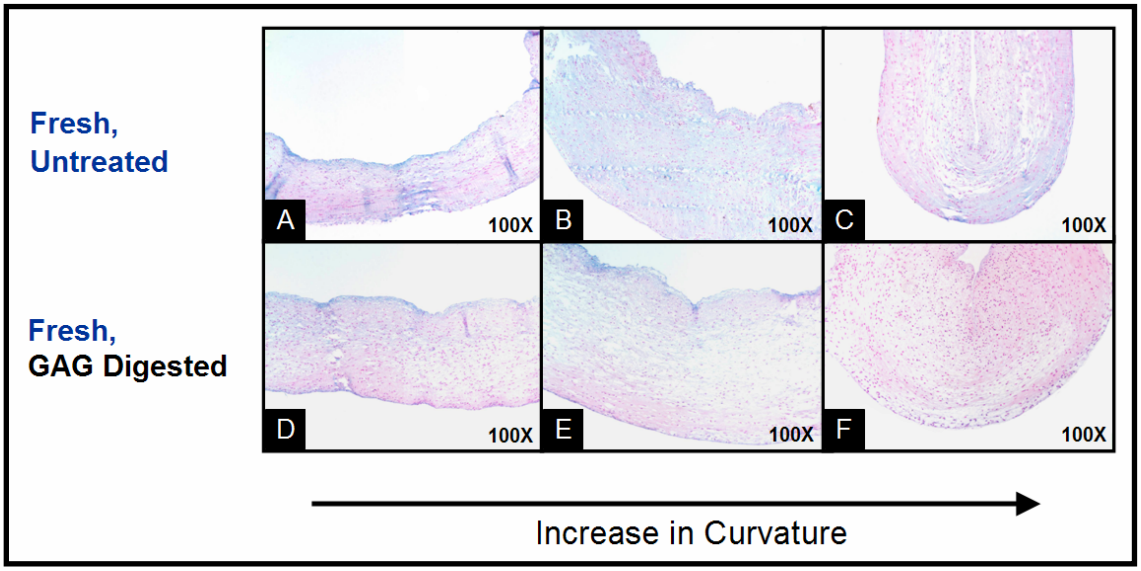

Figure 16: Buckling behavior in fresh cusps: Fresh, unfixed cusps (A-C) without further treatment, and (D-F) with GAG-digestive treatment bent to various curvatures. Curvature of bend increases A to C and D to F. Blue staining using Alcian Blue indicates presence of GAGs.

These results were further confirmed with Hexosamine and DMMB analysis (please refer to proceeding sections) to quantify the retention of GAGs by these cusps whereby glutaraldehyde crosslinked cuspal tissues experienced a decrease in GAG content following treatment with GAG-digestive enzymes ($p<0.05$). Additionally, fresh, untreated cusps exhibited the highest amount of GAGs.

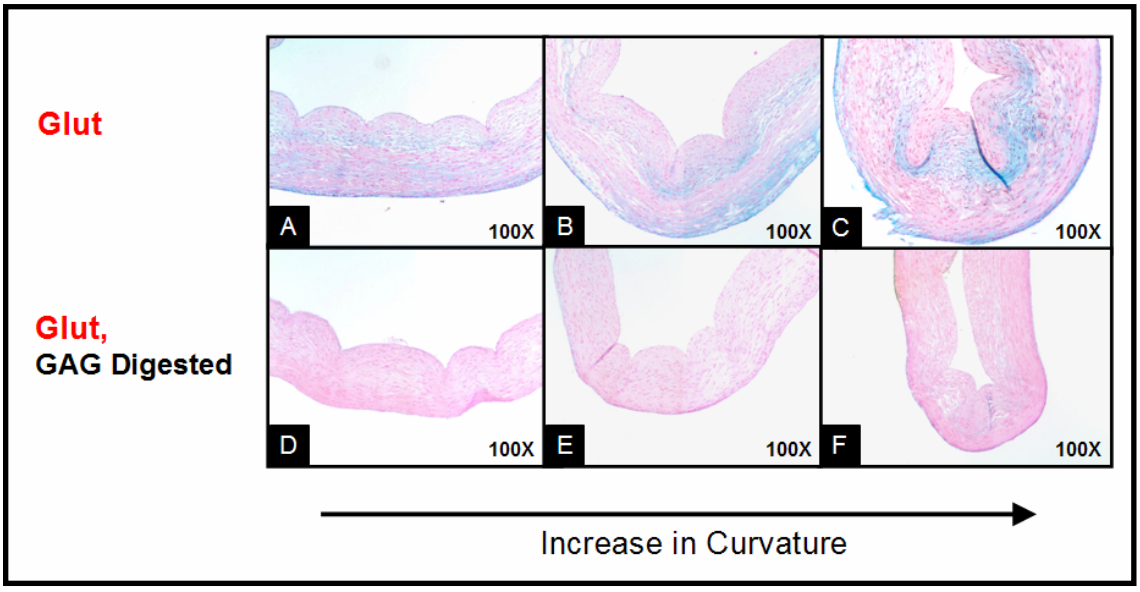

Figure 17: Buckling behavior in cusps pretreated with glutaraldehyde: Glutaraldehyde crosslinked valvular cusps (A-C) without further treatment, and (D-F) with GAG-digestive treatment bent to various curvatures. Curvature of bend increases A to C and D to F. Blue staining using Alcian Blue indicates presence of GAGs.

Hence, to demonstrate these differences graphically, the fractional depth of buckling was plotted against the product of bending curvature and tissue thickness. Due to variability in tissue thickness between each cusp, the bending curvature and tissue thickness were expressed as a product. Also, it must be noted that expressing these two independent variables as a product increased the correlation coefficients of the obtained graphical plots.

In accord with the above-mentioned qualitative observations, similar results were obtained with graphical analyses of the buckling patterns in the aforementioned groups (**Figure 18**).

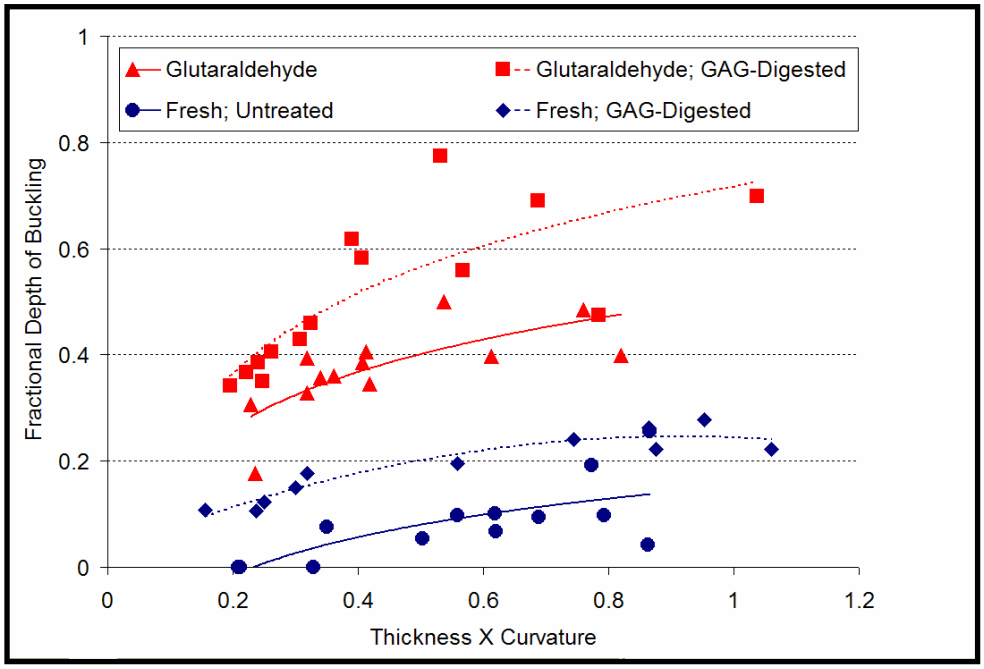

Figure 18: Graphical comparison of buckling pattern in fresh, unfixed and glutaraldehyde pretreated cusps.

In addition, these graphical analyses of buckling behavior suggests that fresh valvular cusps not exposed to any chemical pretreatment experienced relatively mild compressive buckling, with an absence of such tissue deformations at low curvatures. However, glutaraldehyde pretreated cusps experienced a greater depth of buckling at all curvatures, including mild bending curvatures ($p<0.05$). Moreover, when exposed to GAG-digestive enzymes, these glutaraldehyde crosslinked cusps buckled almost through their entire thickness when tightly bent to high curvatures. Conversely, no dramatic increase in buckling pattern was observed in untreated, fresh cusps after treatment with GAG-degrading enzymes. Thus, at all bending radii, the fractional depth of buckling in fresh, untreated cusps significantly differs from cusps pretreated with glutaraldehyde with or without GAG-digestion ($p<0.05$).

To further characterize the surface buckling pattern of the aforementioned treatment groups, the number of surface buckles developed during various cuspal bending radii was quantified. As mentioned previously, both tissue thickness and bending curvature influence the surface buckling pattern of bent cusps. Graphical correlations derived using histological analyses of the buckling outline of bent cuspal tissues verify the aphysiological buckling patterns induced by glutaraldehyde pretreatment and exposure to GAG-digestive enzymes (**Figure 19**).

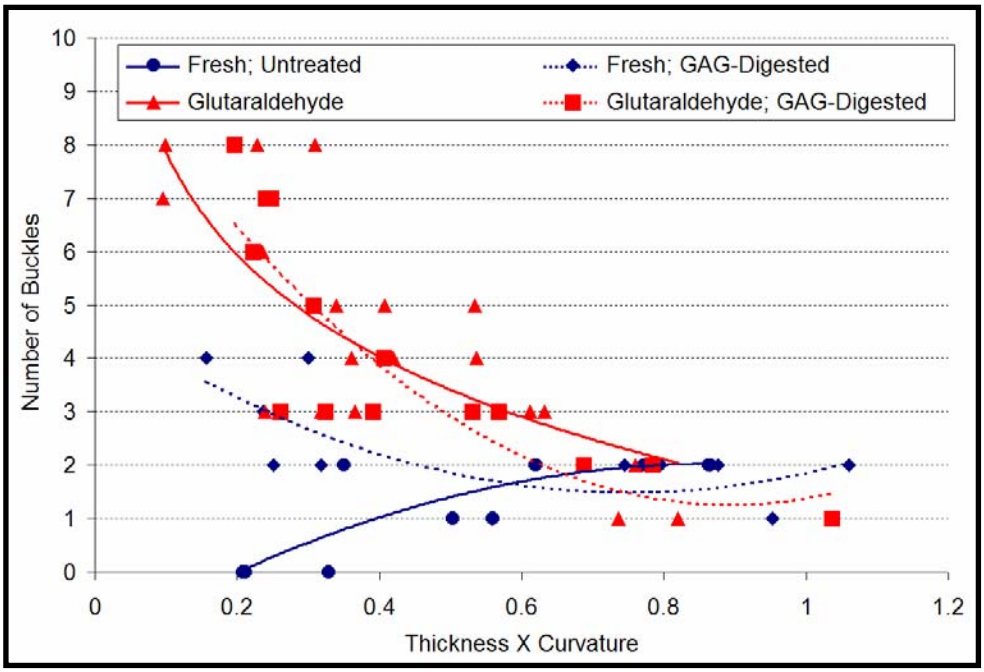

Figure 19: Number of surface buckles produced by fresh, unfixed and glutaraldehyde pretreated cusps at different bending curvatures.

Of particular note, fresh, untreated cusps experienced no buckling at low curvatures; increasing to minimal number of surface buckles at higher bending curvatures. However, cusps pretreated with glutaraldehyde fixation produced numerous

buckles at low curvatures which declined when sharply bent at higher curvatures. Likewise, fresh and glutaraldehyde fixed cusps treated with GAG-degrading enzymes, experienced similar surface buckling outlines. When subjected to sharp bending curvatures, all cuspal groups developed minimal number of surface buckles.

In summary, the following trends were observed: (a) buckling depth increased with increase in curvature; (b) the extent of buckling in glutaraldehyde pretreated cusps was always greater than fresh, unfixed cusps with and without GAG-degrading enzymatic treatment; (c) the loss of GAGs, as observed in these cusps treated with GAG-digestive enzymes, further heightens the extent of buckling; (d) when exposed to glutaraldehyde pretreatment and/or GAG-digestion, the number of buckles developed during low bending curvatures increased compared to fresh, untreated cusps which experienced minimal to no surface buckles at similar high bending radii, (e) however, at higher bending curvatures all cuspal groups produced similar amount of surface buckles.

4.2 The Effect of Glycosaminoglycan-Targeted Fixation Chemistry on Valvular Tissue Buckling

To ascertain the effect of GAG-targeted fixation chemistry on valvular tissue buckling, cusps with bound neomycin trisulfate and those pretreated with EDC/NHS were subjected to different bending curvatures. In addition, both cuspal groups were treated with GAG-digestive enzymes to evaluate the efficacy of the respective GAG-targeted fixation chemistries to retain cuspal GAGs, and thereby reduce the extent of tissue buckling.

Similar to the previous study groups, an increase in buckling depth with an increase in the curvature of the bend was observed (**Figures 20 and 21**). However, unlike glutaraldehyde crosslinked cuspal tissue, cusps pretreated with GAG-targeted fixation chemistries exhibited moderate tissue buckling (**Figures 20 and 21: A, B, C**).

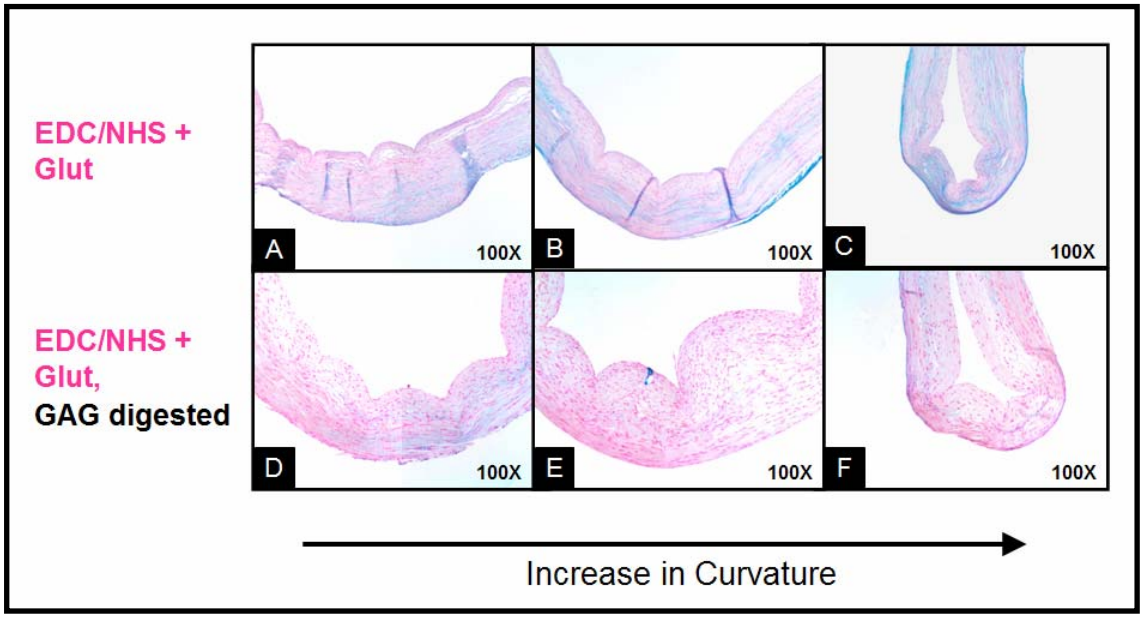

Figure 20: Buckling behavior in cusps exposed to carbodiimide pretreatment: EDC/NHS pretreated cusps (A-C) without, and (D-F) with GAG-digestion bent to various radii. Curvature of bend increases A to C and D to F. Blue staining using Alcian Blue indicates presence of GAGs.

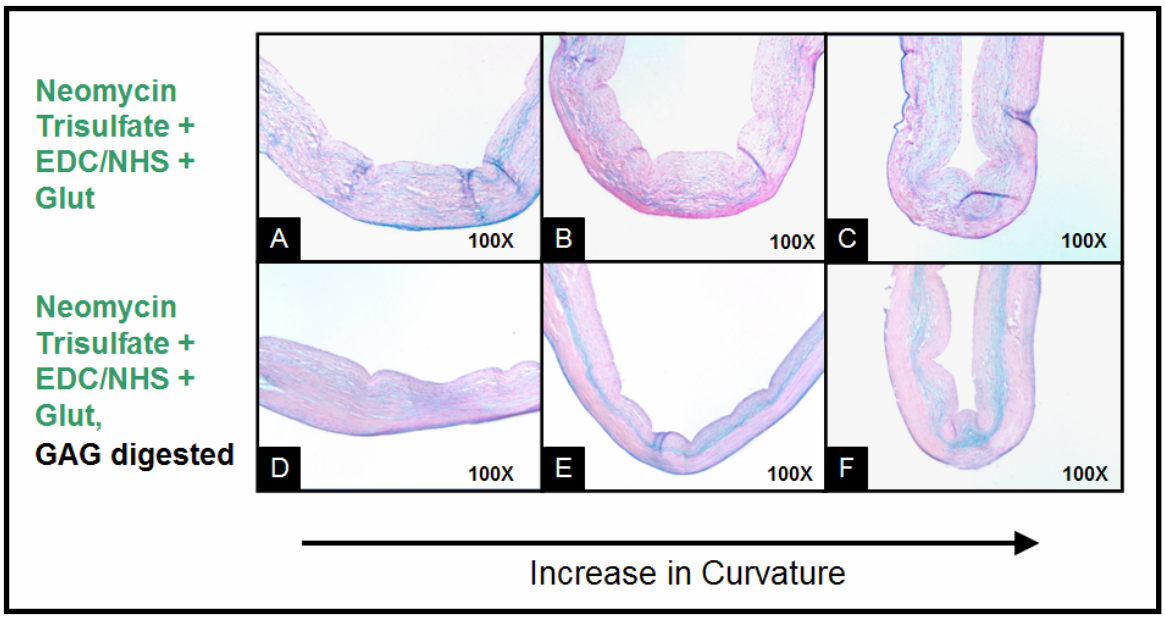

Figure 21: Buckling behavior in cusps with bound neomycin trisulfate: Neomycin trisulfate bound cusps (A-C) prior to, and (D-F) following GAG-digestive treatment bent to various radii. Bending curvature increases A to C and D to F. Blue staining using Alcian Blue indicates presence of GAGs.

Following incubation with GAG-digestive enzymes, cusps exposed to carbodiimide pretreatment alone buckled to a greater extent than prior to such GAG-degrading treatment. Conversely, cusps with bound neomycin trisulfate experienced no significant change in buckling with or without GAG-digestive treatment (**Figure 21**). Alcian blue staining of GAGs indicated almost no change in intensity following enzymatic digestion of GAGs in neomycin trisulfate bound cuspal tissues (**Figure 21**).

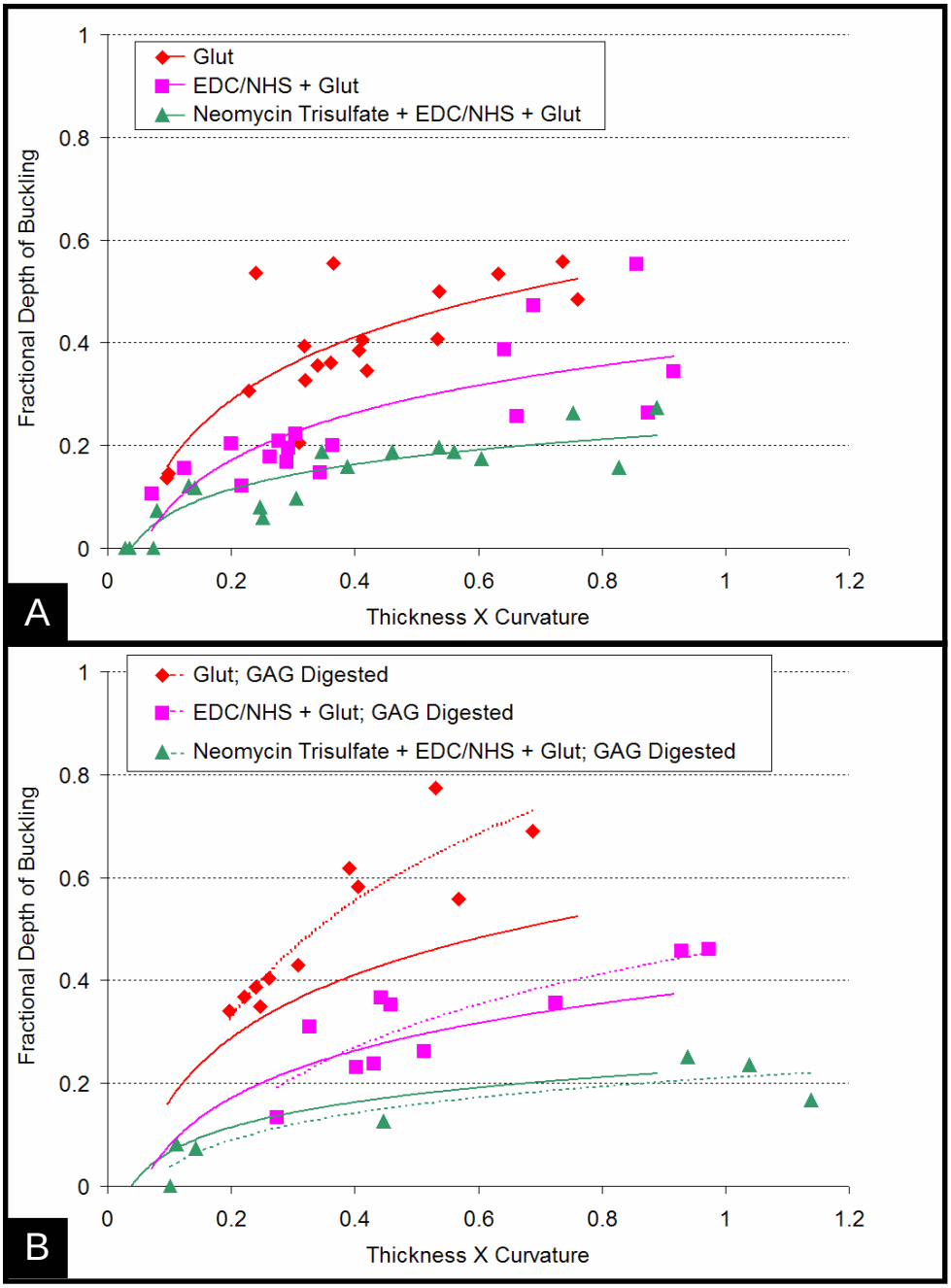

Figure 22: Graphical analyses of valvular tissue buckling in cusps pretreated with glycosaminoglycan-targeted fixation chemistry: (A) prior to, and (B) following incubation with GAG-degrading enzymes.

A quantitative Hexosamine and DMMB assay was conducted (results described in proceeding sections) to verify the efficacy of the GAG-targeted fixation chemistries in the stabilization of valvular GAGs. Neomycin trisulfate pretreated cusps contained the highest amount of GAGs compared to cuspal tissues exposed to other chemical pretreatments. Additionally, following enzymatic digestion, these neomycin trisulfate bound cusps experienced no significant change in GAG content ($p<0.05$).

Furthermore, graphical analyses of the buckling pattern in the aforesaid groups (GAG-targeted fixation chemistries) confirmed the qualitative histological analyses **(Figure 22).** Cuspal tissue bound to neomycin trisulfate experienced the least degree of buckling at all bending curvatures than their glutaraldehyde pretreated counterparts ($p<0.05$) bent to similar configurations (**Figure 22: A**). As indicated in **Figure 22: B**, following GAG-digestive treatment, glutaraldehyde pretreated cusps experienced a greater depth of buckling than neomycin trisulfate treated tissues which exhibited no significant difference in buckling pattern ($p<0.05$). At high curvatures, cusps treated with carbodiimide fixation chemistry alone buckled to a greater extent than those bound with neomycin trisulfate ($p<0.05$).

Upon quantification of the number of buckles produced during various bending radii, it was evident that neomycin bound leaflets experienced minimal to no buckling at low curvatures compared to other chemically pretreated cuspal groups at similar bending curvatures (**Figure 23: A**). However, when subjected to sharp bending radii, all cuspal groups developed analogous amounts of surface buckles.

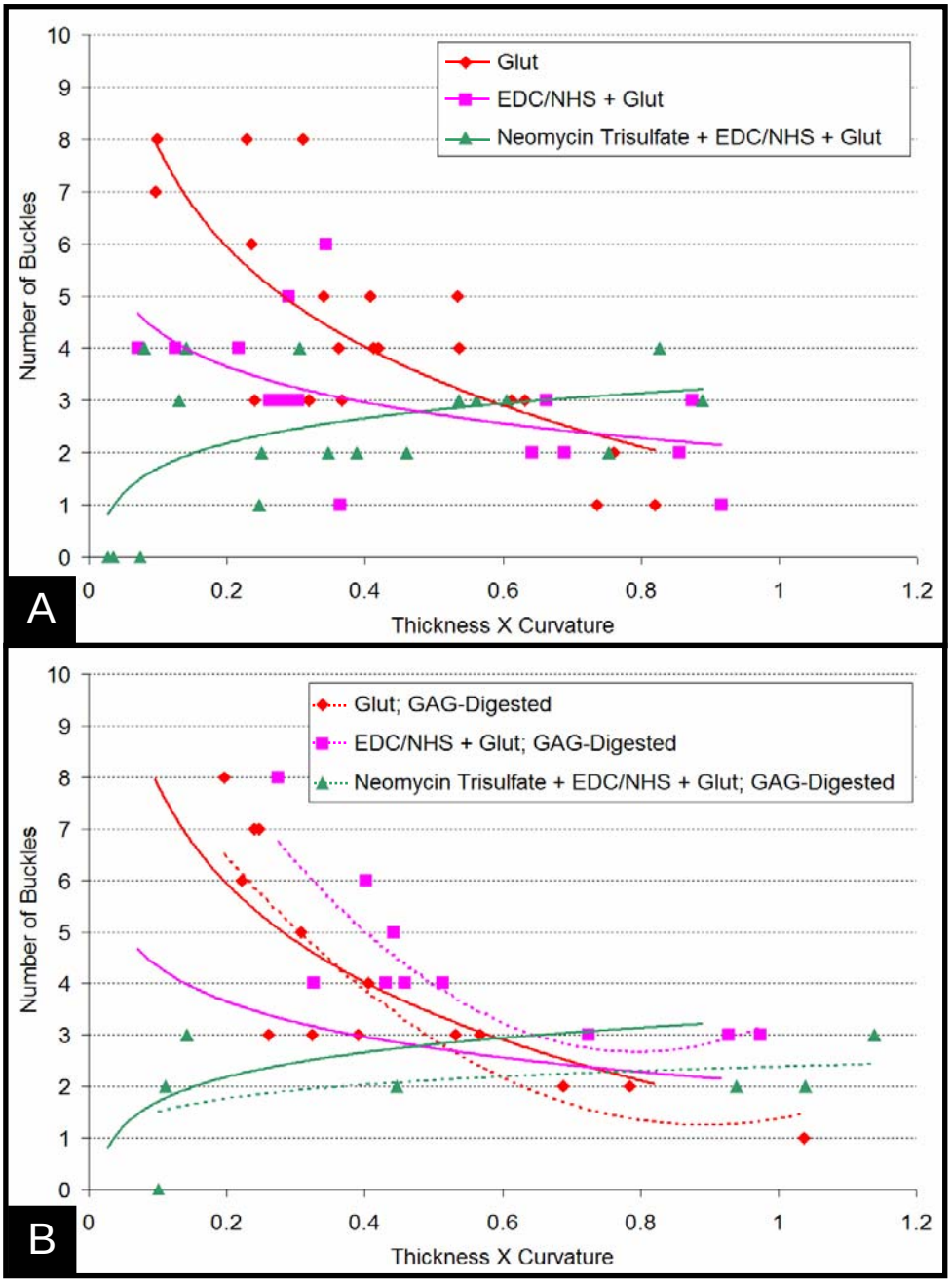

Figure 23: Number of surface buckles produced following bending of cuspal tissue treated with GAG-targeted fixation chemistries: (A) before, and (B) after exposure to GAG-degrading enzymes.

After exposure to GAG-degrading enzymes, all treatment groups produced similar number of buckles when subjected to like bending curvatures (**Figure 23: B**). Particularly noteworthy, cuspal leaflets with bound neomycin trisulfate exhibited similar surface buckling outlines with equivalent number of buckles at all curvatures with or without treatment with GAG-digestive enzymes.

In summation, the following observations are made: (a) tissue buckling depth increased when subjected to high bending curvatures; (b) valvular tissue treated with GAG-targeted fixation chemistries buckled to a lesser extent than cusps crosslinked with glutaraldehyde when subjected to analogous bending configurations; (c) following GAG digestion, cuspal tissue treated with GAG-targeted fixation chemistries showed lesser degree of change in buckling than glutaraldehyde fixed cusps exposed to similar GAG-degrading enzymes; (d) enzymatic digestion of GAGs did not affect the bucking pattern of neomycin trisulfate treated cuspal tissue; (e) neomycin trisulfate bound cusps exhibited the least amount of buckling compared to other chemically fixed tissues, mimicking fresh, untreated cuspal tissue buckling pattern (**Figure 24 A**); (f) furthermore, the number of buckles developed during low bending curvatures in neomycin trisulfate bound cusps with or without exposure to GAG-digestive treatment was minimal compared to the other chemically fixed groups bent to similar radii, mimicking fresh, untreated tissue surface buckling outline (**Figure 24 B**).

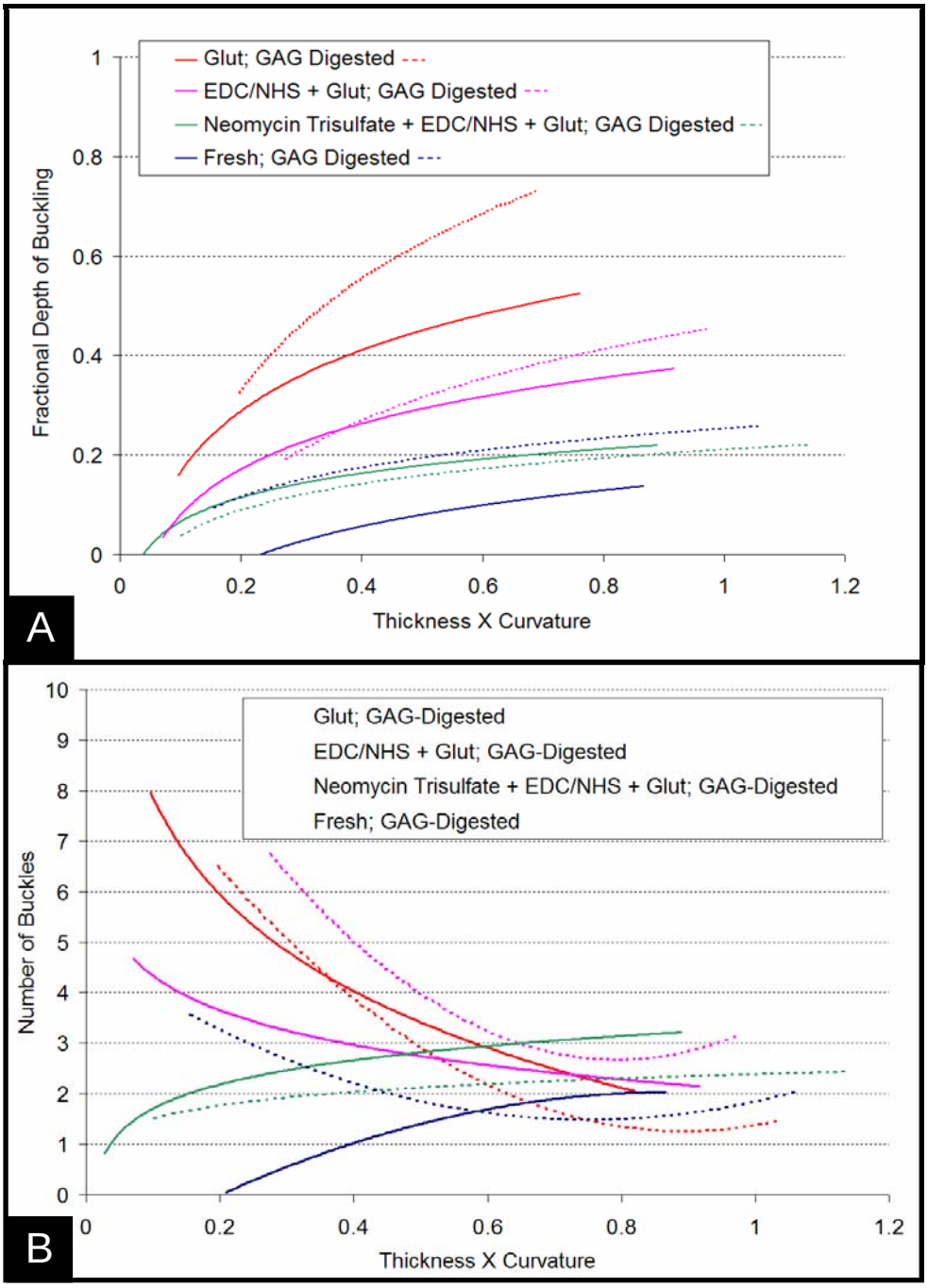

Figure 24: Graphical evaluation of tissue buckling behavior after various chemical pretreatment methods: (A) fractional depth of buckling, and (B) number of buckles.

4.3 Surface Characterization of Valvular Tissue Buckling

The moderate buckling behavior observed in neomycin bound cusps was qualitatively verified by assessing the surface characteristics of the bent cuspal tissue using SEM. Additionally; surface characterization of glutaraldehyde pretreated bent cusps was also conducted to compare such surface differences.

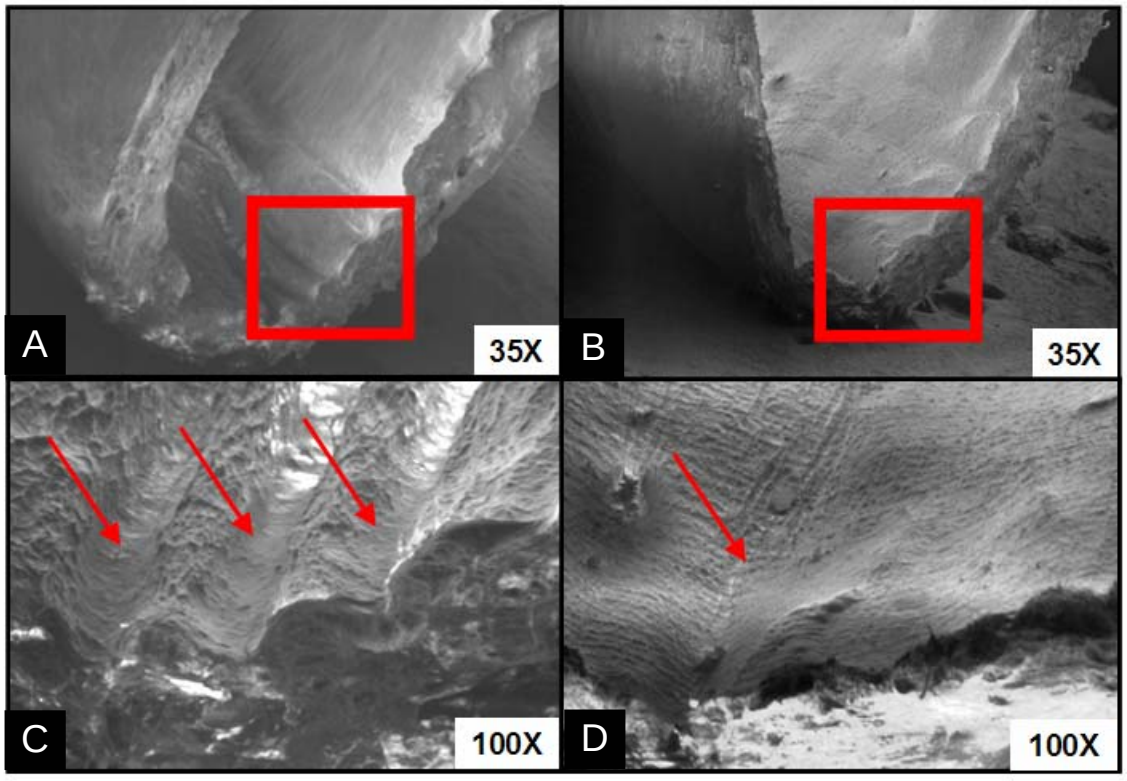

Figure 25: Surface characterization of valvular tissue buckling: (A) glutaraldehyde pretreated cusp and (B) neomycin-trisulfate bound cusp bent to similar curvatures. Images (C) and (D) correspond to magnifications of the highlighted insets of glutaraldehyde pretreated and neomycin-trisulfate bound cusp bent to similar curvatures, respectively. Arrows indicate areas of valvular tissue buckling.

As evident in the SEM images above, surface crimps and kinks were minimal in bent cusps with bound neomycin trisulfate (**Figure 25: A**), while glutaraldehyde

crosslinked cusps exhibited a significant amount of deep creases at similar bending radii, indicating tissue buckling sites (**Figure 25: B**).

Thus, based on the gross appearance of the bent cusps, it can be inferred that cuspal tissue treated with neomycin trisulfate do not produce pronounced surface creases as witnessed in glutaraldehyde crosslinked cusps when subjected to similar bending curvatures.

4.4 The Effect of *In Vitro* Cyclic Fatigue on Valvular Tissue Buckling Behavior Following Treatment with Glycosaminoglycan-Targeted Fixation Chemistry

The efficacy of neomycin trisulfate to resist tissue buckling by stabilizing valvular GAGs was evaluated following *in vitro* cyclic fatigue. To determine the effect of cyclic fatigue on valvular tissue buckling behavior, glutaraldehyde pretreated and neomycin trisulfate bound cusps were subjected to various radii of curvatures after undergoing approximately 10 million accelerated fatigue cycles. Alternatively, another set glutaraldehyde crosslinked and neomycin trisulfate bound valves were stored under static conditions, to discern the change in tissue buckling pattern, if any, due to cyclical fatigue.

Upon histological observations, it was apparent that these cuspal tissues exhibited similar buckling patterns as seen previously (**Figures 26 and 27**). Glutaraldehyde pretreated cuspal tissues experienced a greater depth of buckling at all radii compared to neomycin trisulfate treated cusps. Moreover, glutaraldehyde crosslinked cusps subjected to cyclic fatigue testing buckled to a greater extent than those stored under static conditions when subjected to similar bending configurations. However, no substantial

difference in buckling behavior was observed between neomycin trisulfate bound valvular tissue subjected to fatigue cycling or maintained in a static environment.

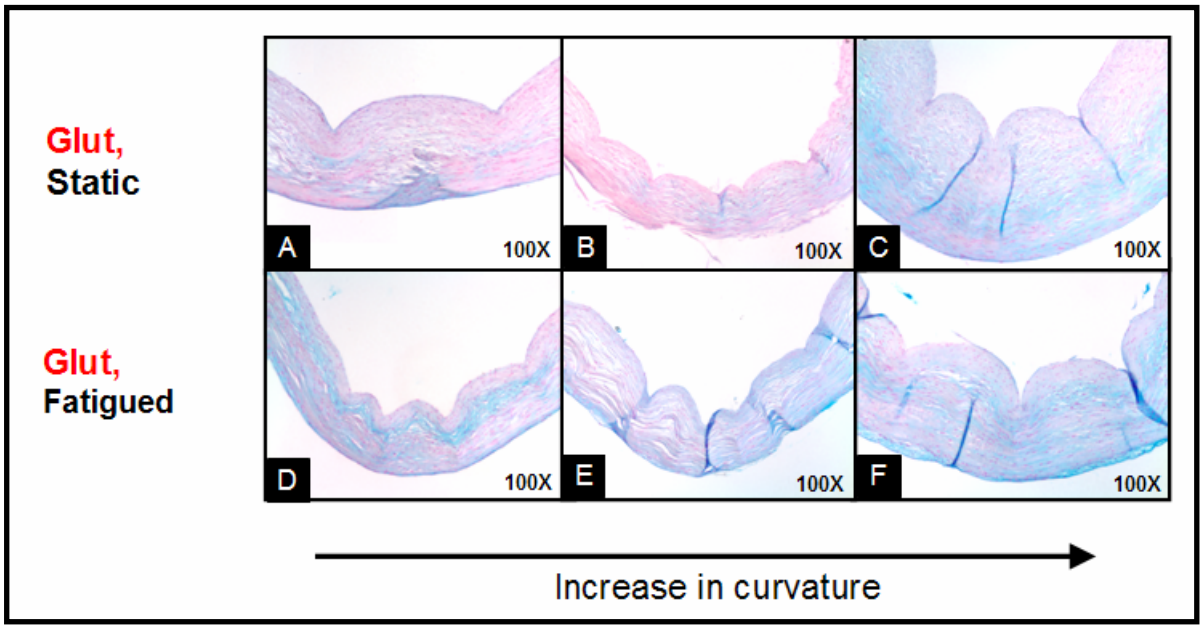

Figure 26: Buckling pattern in glutaraldehyde pretreated cusps following *in vitro* cyclic fatigue: Glutaraldehyde crosslinked cuspal tissue bent to various radii (A-C) following 10 million accelerated fatigue cycles and (D-F) following storage under static conditions. Bending curvature increases A to C and D to F. Blue staining using Alcian Blue indicates presence of GAGs.

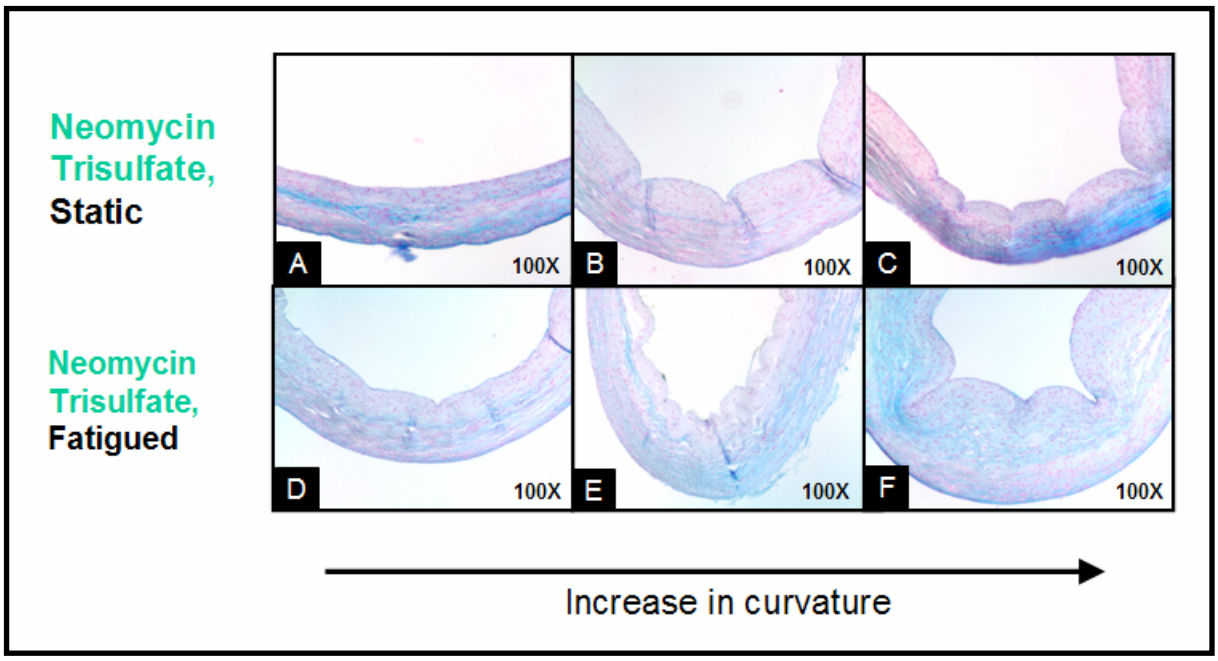

Figure 27: Buckling pattern in neomycin trisulfate bound cusps following *in vitro* cyclic fatigue: Cuspal tissue with bound neomycin trisulfate bent to various radii (A-C) following 10 million accelerated fatigue cycles and (D-F) following storage under static conditions. Bending curvature increases A to C and D to F. Blue staining using Alcian Blue indicates presence of GAGs.

To quantitatively corroborate the abovementioned observations, graphical analyses of the cuspal groups was performed. In concurrence with the qualitative results, analogous tissue buckling behavior was obtained (**Figure 28**), whereby fatigued neomycin trisulfate bound cusps experienced significantly lower fractional buckling depths than glutaraldehyde pretreated cusps with or without cyclical fatigue ($p<0.05$).

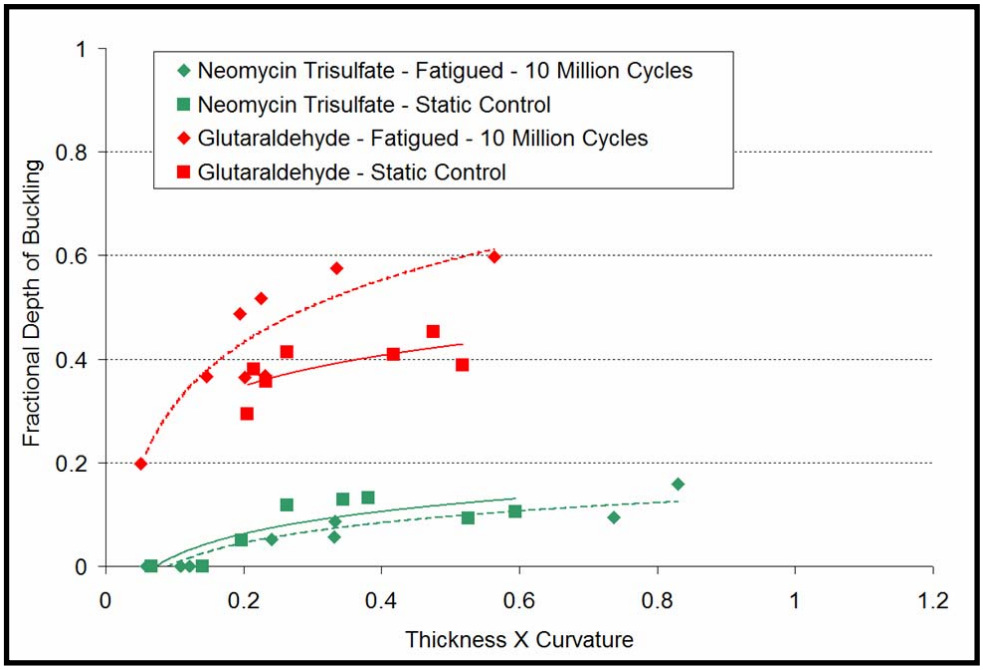

Figure 28: Graphical assessment of buckling behavior of *in vitro* cyclic fatigued cusps.

To further characterize the buckling pattern of these cyclical fatigued tissues, the number of buckles produced by these cusps when subjected to different bending radii was evaluated (**Figure 29**). An absence of buckles was observed at low curvatures in cusps bound with neomycin trisulfate subjected to cyclical fatigue, mimicking statically stored cusps. However, glutaraldehyde pretreated cusps experienced increased amount of buckles at such bending radii. When subjected to sharp bending curvatures, all cuspal groups exhibited equivalent number of surface buckles.

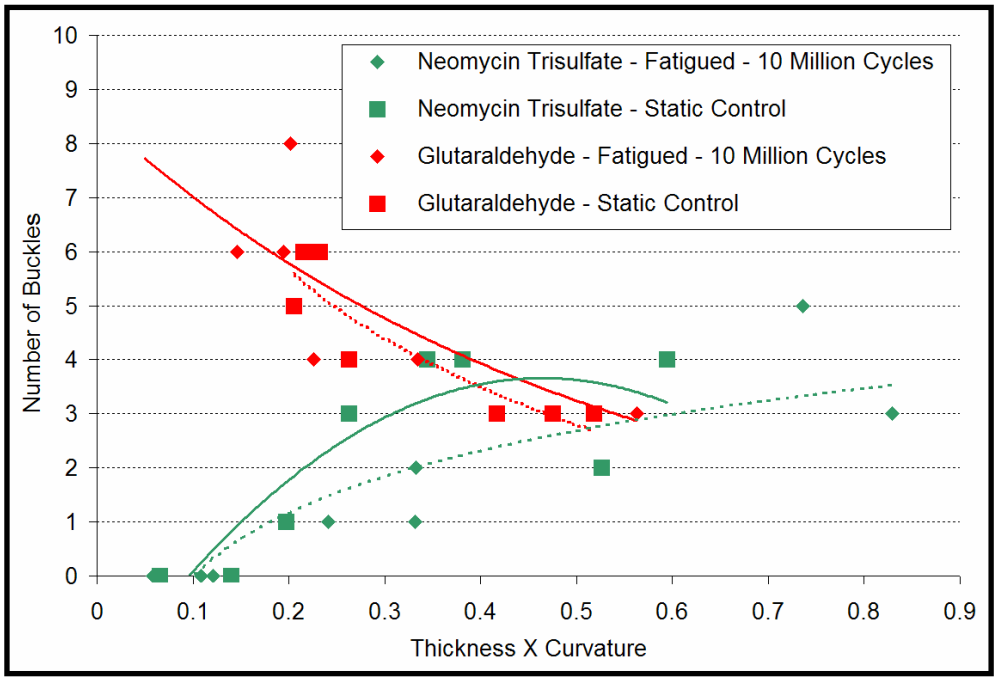

Figure 29: Graphical assessment of surface buckling outline of *in vitro* cyclic fatigued cusps at various bending radii.

Thus, based on these results, the following observations can be summarized: (a) as seen previously, buckling depth increased with an increase in bending curvatures; (b) glutaraldehyde pretreated cusps subjected to cyclical fatigue testing buckled to a greater degree than valvular tissue bound with neomycin trisulfate and exposed to likewise accelerated fatigue conditions; (c) fatigue cycling of neomycin trisulfate bound cuspal tissue experienced no deviations in buckling pattern than those cusps not exposed to such treatment and instead maintained in a static environment; and (d) tissue buckling behavior of these neomycin bound cusps parallels fresh, untreated valvular tissue buckling pattern.

4.5 Efficacy of Glycosaminoglycan-Targeted Fixation Chemistry to Resist Enzymatic Degradation of Glycosaminoglycans

The efficacy of GAG-targeted fixation chemistries to prevent enzymatic degradation of GAGs was quantified by treating crosslinked cuspal tissue with GAG-degrading enzymes (namely, hyaluronidase and chondroitinase) and comparing their GAG content to crosslinked cusps not exposed to any GAG-digestive treatments. Following the above-mentioned treatments, Hexosamine analysis indicated the highest loss of GAGs ($p<0.05$) in glutaraldehyde crosslinked cusps after enzymatic digestion **(Figure 30)**, similar to fresh, untreated cusps ($p>0.05$). Cusps exposed to GAG-targeted fixation chemistry exhibited the highest resistance to enzymatic removal of GAGs ($p<0.05$). Also, cuspal groups pretreated with glutaraldehyde and EDC/NHS showed no statistical difference between their GAG content values ($p<0.05$). Of all the three cuspal fixation groups, neomycin trisulfate bound cusps retained the highest amount of GAGs prior to and following digestion ($p<0.05$), mimicking fresh, untreated cusps ($p>0.05$). These results indicate the effectiveness of bound neomycin trisulfate using GAG-targeted fixation chemistry to prevent the enzymatic removal of GAGs. Additionally, GAG content in glutaraldehyde and EDC/NHS crosslinked cusps was significantly ($p<0.05$) lower before enzymatic digestion than compared to neomycin trisulfate bound cusps prior to or following GAG-digestion, indicating the instability of GAGs in the aforementioned cuspal treatment groups.

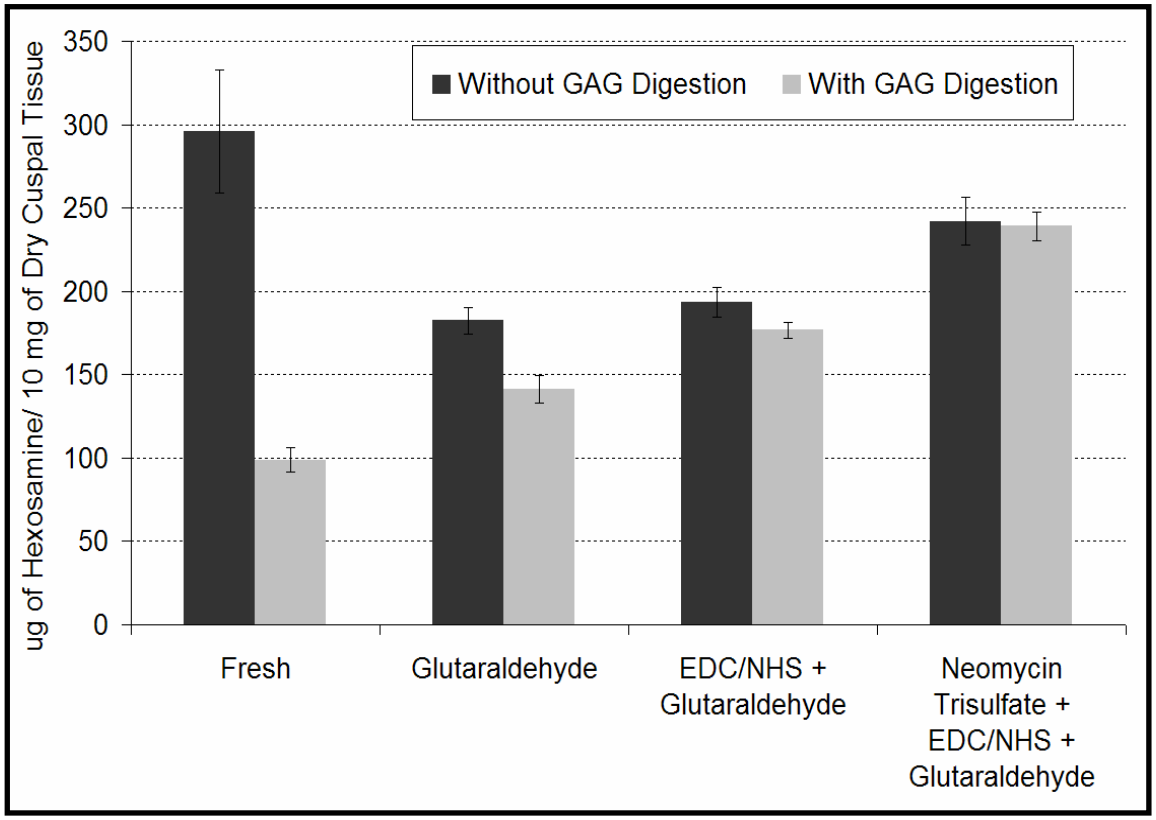

Figure 30: Valvular glycosaminoglycan retention prior to and following pretreatment with glutaraldehyde and glycosaminoglycan-targeted fixation chemistries.

To further quantify the loss of GAGs in the crosslinked cuspal tissue prior to and following GAG-digestive treatments, the respective buffer and enzyme solutions of each group were analyzed for released GAGs by DMMB assay (**Figure 31**). Significantly higher GAG content ($p<0.05$) was detected in the enzyme solutions of GAG-digested glutaraldehyde and EDC/NHS pretreated cusps; while an insignificant amount ($p<0.05$) of GAGs were released into the buffer and enzyme solutions of cuspal tissue with bound neomycin trisulfate.

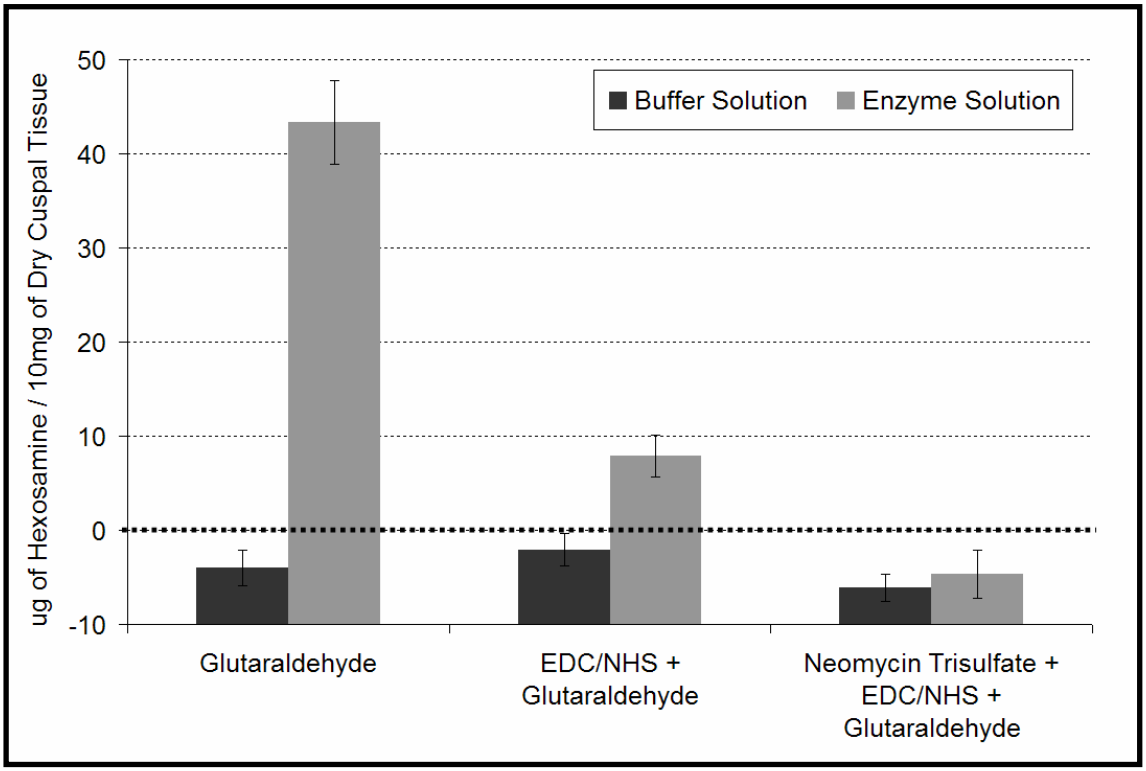

Figure 31: Loss of glycosaminoglycans following pretreatment with glutaraldehyde and glycosaminoglycan-targeted fixation chemistries.

These results indicate that almost complete resistance to GAG-degrading enzymes by cuspal GAGs is achieved by binding neomycin trisulfate to these cusps. Such binding inhibits the effectiveness of GAG-digestive enzymes (namely, hyaluronidase and chondroitinase) to degrade cuspal GAGs.

4.6 Effect of Glycosaminoglycan-Targeted Fixation Chemistry on Cuspal Water Content and Rehydration Capacity

To evaluate the effect of the GAG-targeted fixation methods on cuspal hydration, the water content of each cuspal treatment group was measured. Following the appropriate fixation methods, glutaraldehyde crosslinked cuspal tissue exhibited

significantly higher water content ($p<0.05$) than compared to those cusps treated with GAG-targeted fixation chemistries.

Furthermore, the water content of each cuspal fixation group was quantified following treatment with GAG-degrading enzymes to correlate cuspal hydration with GAG stabilization. As evident in **Figure 32**, glutaraldehyde pretreated cusps exhibited the greatest reduction in hydration capacity following enzymatic removal of GAGs ($p<0.05$). Despite their reduced hydration capacity prior to GAG-digestive treatment, cusps exposed to GAG-targeted fixation chemistries did not demonstrate a significant loss of water content after such enzymatic treatment. As previously mentioned, EDC/NHS treated and neomycin trisulfate bound cusps maintained significantly higher GAG content following GAG digestion than compared to glutaraldehyde pretreated valvular tissues ($p<0.05$). Thus, GAG stabilization using GAG-targeted fixation chemistries maintained hydration capacities of cuspal tissues regardless of exposure to GAG-digestive enzymes.

Additionally, the rehydration capacity of crosslinked cusps was assessed prior to and following treatment with GAG-digestive enzymes. Glutaraldehyde pretreated cusps were unable to fully rehydrate while cusps treated with GAG-targeted fixation chemistries exhibited a higher capacity to rehydrate. Moreover, neomycin trisulfate bound cusps rehydrated to their full capacity without any significant change in water content ($p<0.05$) before and after GAG-digestive treatment. Conversely, cusps exposed to glutaraldehyde pretreatment significantly lost additional rehydration capacity following treatment with GAG degrading enzymes ($p<0.05$).

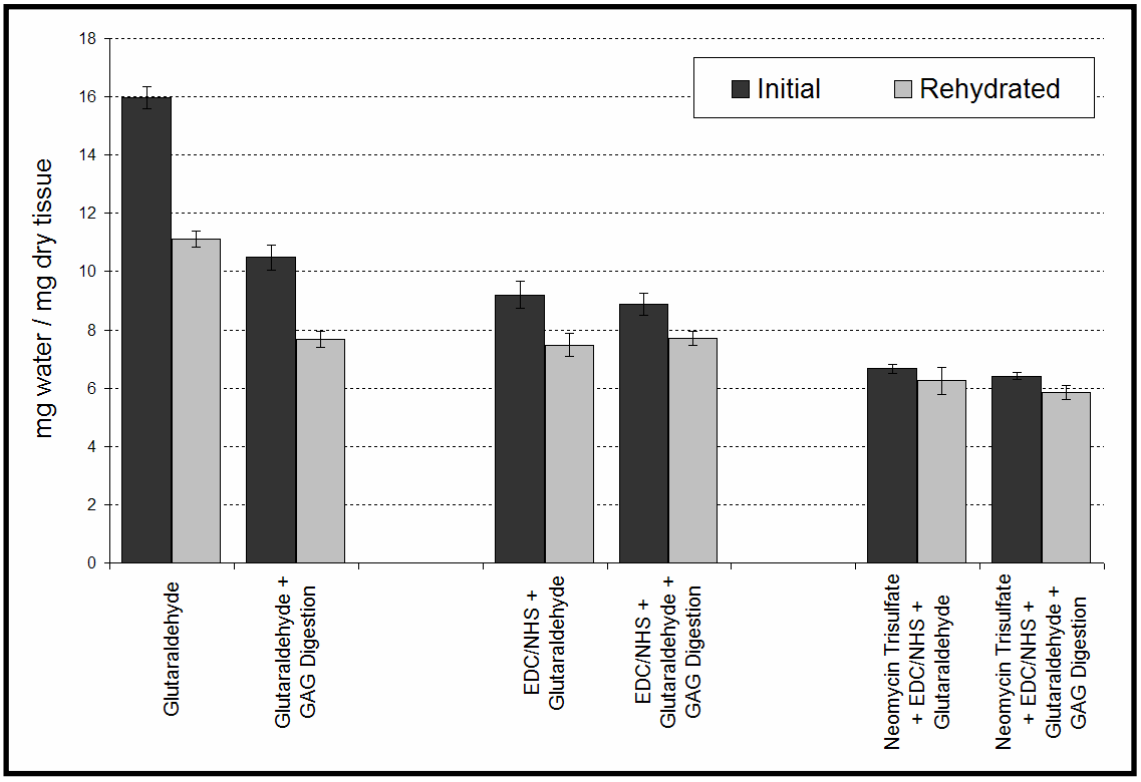

Figure 32: Water content and rehydration capacity of valvular tissue following pretreatment with glutaraldehyde and glycosaminoglycan-targeted fixation chemistries.

Thus, these results indicate that stabilization of GAGs using neomycin trisulfate enables cuspal tissues to maintain their hydration status regardless of exposure to GAG-digestive enzymes. Furthermore, cuspal tissue treated with neomycin trisulfate does not demonstrate a change in water content following rehydration. Likewise, treatment with GAG-degrading enzymes does not alter the aforementioned rehydration capacity of neomycin trisulfate bound cusps.

CHAPTER 5

DISCUSSION

Valvular tissue buckling, one of the causes of failure in bioprosthetic heart valves, has been implicated in the evolution of fatigue failure in these bioprostheses. Characterized by surface deformations, buckling occurs at areas of large stresses during valvular motion. During diastole, valvular xenografts are subjected to uniaxial compression due to sharp bending in the belly and commissural regions of the cusps [5, 6, 121]. Such valvular behavior produces surface kinks and crimps, resulting in local structural collapse to reduce the bending stresses. Upon initiation of buckling, such tissue bending deformations continue to occur in the same area during each successive valvular cycle. Consequentially, the bending site fatigues, leading to subsequent tearing of the cusps.

5.1 Role of Glycosaminoglycans in Valvular Tissue Buckling

During diastolic motion, valvular cusps are subjected to compressive, tensile, and shear stresses. By dissipating shear stresses, the medial spongiosa layer, rich in GAGs, buffers the appositional movement of the outer layers which are subjected to tensile and compressive loads. These hydrophilic GAGs form a gel-like layer, capable of absorbing such stresses during valvular bending.

Conventional glutaraldehyde crosslinking of porcine aortic valves does not provide complete stabilization of valvular extracellular matrix. Plagued by its inability to

stabilize valvular GAGs, conventional glutaraldehyde crosslinking of porcine aortic heart valves does not maintain native shear properties of the valve, partially due to the leaching of GAGs [24, 25, 91, 119].

The pronounced depth and amount of buckling observed in glutaraldehyde pretreated valvular cusps is attributed to the loss of GAGs and stiffness imparted by such collagenous crosslinking. Unable to hydrate the valvular tissue, coupled with the relative loss of flexibility, these glutaraldehyde pretreated cusps buckle. However, untreated cusps do not exhibit such abnormal bending behavior. Their intact tri-layered structure endows these cusps their pliable character to resist compressive buckling during successive bending cycles.

Due to the absence of amine functionalities in GAGs, glutaraldehyde treatment is unable to stabilize valvular GAGs. Thus, the ineffectiveness of the glutaraldehyde to crosslink GAGs, permits exogenous GAG-degrading enzymes access to cleavage sites. Previous studies propose that carboxylic sites present on uronic acids of GAGs activate the degradation of glycosidic bonds in GAGs by hyaluronidase and chondroitinase. Additionally, non-reducing terminal GAG residues are susceptible to biodegradation by glucoronidase. Similarly, degradation of the protein core of GAGs is facilitated by the action of matrix metalloproteinase (MMP). These enzymes are also implicated in collagen fiber disruption which leads to further loss of valvular structural integrity. Thus, following GAG-digestive treatment, glutaraldehyde crosslinked cuspal tissue, depleted of valvular GAGs, experienced a greater degree of valvular tissue buckling.

Therefore, by maintaining a hydrated environment necessary for absorbing compressive loads, dissipating shear stresses, and resisting tissue buckling, GAGs preserve the durability of heart valves.

5.2 Stabilization of Glycosaminoglycans to Reduce Valvular Tissue Buckling

Chemical stabilization of valvular GAGs does not prevent enzymatic degradation of these extracellular matrix components. A recent study reported the use of neomycin trisulfate, a hyaluronidase inhibitor, coupled with carbodiimide based crosslinking chemistry to effectively stabilize valvular GAGs [10]. Such GAG-targeted fixation chemistry utilizes the presence of amine functionalities present in neomycin trisulfate to chemically bind to carboxylic groups of GAG uronic acids by carbodiimide crosslinking [10]. Under acidic conditions, activation of carboxyl groups of the uronic acids present in GAG disaccharide molecules by EDC promotes N-hydroxysuccinimide (NHS) to react with GAGs, forming unstable intermediates. These intermediates form “zero-length” crosslinks with the free amine groups of collagen via amide bonds [125]. Neomycin trisulfate, a sulfated oligosaccharide containing primary amine groups, has a combination of hydrophilic moieties with affinity-conferring lipophilic residues that bind to hyaluronidase to prevent enzymatic degradation of GAGs [126]. Thus, when coupled with carbodiimide fixation chemistry, the amine functionalities of neomycin trisulfate form amide bonds with the carboxylic groups of GAGs [10].

Valvular cusps with bound neomycin trisulfate inhibited enzyme-mediated GAG degradation. Additionally, these GAG-stabilized cusps exhibited the least amount and

extent of buckling, mimicking fresh untreated tissue buckling behavior. The hydrophilic moieties with an affinity-conferring lipophilic residues present in sulfated neomycin molecules (**Figure 33**) bind to hyaluronidase; and thus, block enzymatic activity [126].

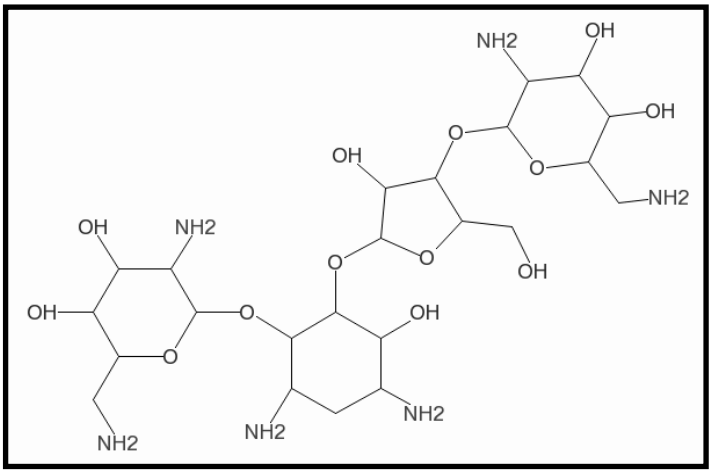

Figure 33: Chemical structure of neomycin trisulfate. This hyaluronidase inhibitor contains 6 primary amine groups that chemically attach to cusp proteins with carbodiimide chemistry.

Such binding renders the enzyme inactive. Stabilization of GAGs is achieved by coupling neomycin trisulfate with carbodiimide fixation. Activation of carboxylic groups of GAGs and collagen by EDC enables formation of a stable intermediate with NHS, and subsequent amide bonding with free amine groups of collagen [125]. Thus, such GAG-targeted fixation chemistry facilitates the maintenance of valvular shear properties by the stabilization of GAGs; thereby reducing the extent of buckling.

As mentioned previously, the carboxylic functionalities of GAGs are active sites for enzymatic degradation. Carbodiimide fixation is partially effective in stabilization of GAGs due to its inability to crosslink all valvular carboxylic groups [47, 127]. Thus, due

to the partial loss of GAGs, these cusps experience a moderate depth of buckling than those cusps pretreated with glutaraldehyde.

However, cuspal tissues with bound neomycin trisulfate exhibited the least amount of buckling. Such enzyme inhibition and GAG crosslinking by carbodiimide fixation prevents additional GAG loss. Thus, neomycin trisulfate not only blocks active sites on GAGs, but confers GAG-digestive enzymes inactive by binding to GAG-degrading enzymes. Steric hindrance of the active site and conformational change of the enzyme precludes loss and digestion of GAGs, which reduces the extent of buckling.

Furthermore, neomycin trisulfate bound cusps exhibited almost complete resistance to GAG-degrading enzymes, while carbodiimide fixation alone was shown to partially inhibit GAG-digestion. Likewise, cuspal tissue exposed to this enzyme inhibitor experienced no change in buckling behavior after exposure to GAG-digestive enzymes. However, glutaraldehyde treated cusps which are ineffective at stabilizing valvular GAGs, demonstrated the greatest depth of buckling at all curvatures and significant number of buckles at low curvatures following incubation with GAG-degrading enzymes.

Thus, stabilization of GAGs by neomycin trisulfate coupled with carbodiimide fixation chemistry precludes valvular tissue buckling. The presence of valvular GAGs appropriates the cusp its structural and functional integrity necessary to resist compressive buckling during bending.

5.3 Resistance of Neomycin Trisulfate-Enhanced Glycosaminoglycan-Targeted Crosslinking to Tissue Buckling in Fatigued Valves

Stabilization of cuspal GAGs during cyclical motion of the valve will permit enhanced durability of the valves. During the cardiac cycle, valvular cusps are continuously subjected to tensile, compressive, and shear stresses. The interlayer shearing between the fibrosa and ventricularis is mediated by the medial spongiosa layer. Particularly, GAGs, hydrophilic in nature, form a gel-like layer in the spongiosa capable of distributing and dissipating these valvular stresses.

Ongoing studies indicate that the stabilization of valvular tissue by neomycin trisulfate binding to resist depletion of GAGs during *in vitro* cyclic fatigue testing. On the contrary, glutaraldehyde pretreatment does not stabilize valvular GAGs, necessary for maintaining cuspal mechanical durability during such cyclical testing [4]. Current studies demonstrate no difference in buckling behavior in neomycin trisulfate bound cuspal tissue after accelerated fatigue testing than compared to buckling patterns of statically stored valves. Additionally, these GAG-stabilized cusps exhibited minimal fractional depth of buckling compared to glutaraldehyde pretreated valves which are prone to GAG loss during similar fatigue testing. Moreover, glutaraldehyde crosslinked valves exhibited a greater depth of buckling post-*in vitro* cyclic fatigue than compared to those pretreated cusps stored under static conditions. Interestingly, fatigued neomycin trisulfate treated tissues maintained minimal amounts of surface buckles as observed in cusps stored under static conditions, mimicking fresh, untreated cuspal buckling behavior.

Thus, valvular cusp's ability to flexibly deform during successive valve cycles, absorb compressive loads during diastolic closing, and dissipate shear stresses

experienced during valvular motion are largely possible due to the presence of GAGs in the medial spongiosa layer. Moreover, neomycin trisulfate-enhanced carbodiimide mediated crosslinking precludes valvular tissue buckling when subjected to short-term cyclic fatigue testing compared to commercially available glutaraldehyde fixation. Therefore, stabilization of valvular GAGs using neomycin trisulfate coupled with carbodiimide fixation chemistry improves the buckling behavior of these cusps following cyclical fatigue.

5.4 Efficacy of Glycosaminoglycan-Targeted Fixation Chemistry to Maintain Valvular Hydration Properties

Cuspal hydration plays an important role in physico-mechanical properties of valves. Specifically, water-absorbing GAGs predominantly present in the spongiosa, maintain the internal shear properties of the valvular tissues. These hydrophilic molecules facilitate proper appositional sliding of the two outer layers by formation of a gel-like environment necessary to resist tensile and compressive stresses. Thus, maintenance of valvular GAGs improves bending pattern of cuspal tissues, and subsequently precludes abnormal buckling behavior.

Present studies indicate a decline in water content following crosslinking with GAG-targeted fixation methods compared to conventional glutaraldehyde pretreatment. One plausible explanation of this decay in hydration status of the cusps is due to the reduction of available hydrophilic GAG moieties which are crosslinked with GAG-stabilizing fixatives. Unable to access these GAG carboxylic binding groups, the bound water content of the valvular cusps diminishes. Additionally, the heavy crosslinking

induced by chemical fixation decreases the amount of cuspal bulk water, which may predominantly account for the observed regression in overall water content of cuspal tissues. However, future studies must be conducted to verify this difference in hydration status of the aforementioned valvular cusps. Of particular note, biomechanical behavior is primarily influenced by bound water.

Loss of cuspal GAGs following enzymatic digestion resulted in a decrease in water content. However, neomycin trisulfate bound cusps protected against such GAG-degrading activity displayed no significant difference in water content. Additionally, these cusps rehydrated to their full capacities while the other fixation methods experienced a loss in rehydration capacity.

Future studies must be conducted to quantify the amount of cuspal bound water to accurately infer its implications on biomechanical properties of valvular tissues.

CHAPTER 6

CONCLUSIONS AND RECOMMENDATIONS

6.1 Conclusions

Despite numerous advances in the design of BHVs, the durability of these bioprostheses is limited due to dysfunction, and subsequent degeneration. Partly owing to the structural demands imposed by the cardiac system, stabilization of the morphological properties of valvular cusps may ultimately enhance the long-term performance and efficiency of these implants.

Current fixation strategies fail to stabilize extracellular matrix components of the valves, particularly GAGs, essential for maintaining a hydrated environment necessary for absorbing compressive loads, dissipating shear stresses, and resisting tissue buckling. Present studies demonstrate the efficacy of neomycin trisulfate, a GAG-digestive enzyme inhibitor, coupled with carbodiimide fixation to stabilize valvular GAGs and subsequently resist tissue buckling. Alternatively, glutaraldehyde pretreated and carbodiimide crosslinked cusps, which are susceptible to enzymatic degradation of GAGs, exhibit an increased fractional depth of buckling at all curvatures and are not immune to elevated buckling patterns following cyclic fatigue due to the loss of valvular GAGs. Additionally, cuspal tissue pretreated with commercially available glutaraldehyde bucked to the greatest extent than compared to the other groups.

Therefore, in summation the following conclusions can be inferred from the present results: (a) valvular GAGs play a role in resisting tissue buckling; (b) stabilization

of valvular GAGs using neomycin trisulfate-enhanced carbodiimide mediated crosslinking precludes tissue buckling; (c) exposure to GAG-degrading enzymes does not alter the buckling behavior of neomycin trisulfate bound cuspal tissues; (d) likewise no change in buckling pattern is observed following short-term *in vitro* cyclic fatigue testing of neomycin trisulfate bound cusps; and furthermore, (e) valvular tissue buckling pattern observed in these GAG-stabilized cusps mimic fresh cuspal buckling behavior.

Thus, stabilization and retention of valvular GAGs using GAG-targeted fixation chemistries may in fact reduce the extent of buckling in BHVs and subsequently improve the durability of these bioprostheses.

To ensure the durability of BHVs, the structural and functional attributes of valvular tissue must be maintained. Due to their inherent biological similarities with native valvular cusps, porcine-derived BHVs constructs have the ability to support natural and physiologically relevant hemodynamic and hydrodynamic flow regimes. Furthermore, by optimizing their morphological properties, these bioprostheses may qualify as a suitable replacement modality with extended biological and mechanical durability.

6.2 Recommendations

Future studies are warranted to continue to examine the efficacy of GAG-targeted fixation chemistries to resist valvular tissue buckling in long-term accelerated fatigue tested cusps. Additionally, it is necessary to understand the changes in the mechanical properties of these GAG-stabilized valvular tissues in order to design durable substitutes.

As such, internal shear properties of the cusps must be examined to correlate the tissue buckling behavior with GAG content, hydration status, and flexural testing. Furthermore, to ascertain the relationship between compressive buckling and internal shearing, other useful parameters such as viscoelastic behavior, rigidity, and effective stiffness during dynamic flexure must be explored.

As mentioned previously, besides non-calcific structural damage, calcification of the valves *in vivo* imposes another potential threat to the durability of these bioprostheses. Thus, future studies should focus on coupling neomycin trisulfate-enhanced GAG-targeted fixation chemistry with anti-calcification treatments capable of sustaining the physico-mechanical character of valvular tissues. Additionally, by examining buckling patterns in such valvular cusps, degenerative culprits responsible for undermining the long-term mechanical durability of these valves can be identified.

Thus, by understanding the role of GAGs in cuspal tissue buckling, the mechanical properties of the valvular constructs can be improved. Furthermore, investigation of potential correlates of cuspal deformations can enhance our abilities to halt the evolution of fatigue and subsequent tearing of the cusps, and thus, extend the functional life of porcine-derived BHVs. These strides in research will contribute to the overall development of biomechanically stable valvular substitutes capable of withstanding long-term implantation.

REFERENCES

1. Everaerts, F., et al., *Reduced calcification of bioprostheses, cross-linked via an improved carbodiimide based method.* Biomaterials, 2004. **25**(24): p. 5523-30.

2. Schoen, F.J. and R.J. Levy, *Founder's Award, 25th Annual Meeting of the Society for Biomaterials, perspectives. Providence, RI, April 28-May 2, 1999. Tissue heart valves: current challenges and future research perspectives.* J Biomed Mater Res, 1999. **47**(4): p. 439-65.

3. Lovekamp, J.J., et al., *Stability and function of glycosaminoglycans in porcine bioprosthetic heart valves.* Biomaterials, 2006. **27**(8): p. 1507-18.

4. Vyavahare, N., et al., *Mechanisms of bioprosthetic heart valve failure: fatigue causes collagen denaturation and glycosaminoglycan loss.* J Biomed Mater Res, 1999. **46**(1): p. 44-50.

5. Vesely, I., D. Boughner, and T. Song, *Tissue buckling as a mechanism of bioprosthetic valve failure.* Ann Thorac Surg, 1988. **46**(3): p. 302-8.

6. Vesely, I. and W.J. Mako, *Comparison of the compressive buckling of porcine aortic valve cusps and bovine pericardium.* J Heart Valve Dis, 1998. **7**(1): p. 34-9.

7. Mercuri, J.J., et al., *Glycosaminoglycan-targeted fixation for improved bioprosthetic heart valve stabilization.* Biomaterials, 2007. **28**(3): p. 496-503.

8. Simionescu, D.T., J.J. Lovekamp, and N.R. Vyavahare, *Extracellular matrix degrading enzymes are active in porcine stentless aortic bioprosthetic heart valves.* J Biomed Mater Res A, 2003. **66**(4): p. 755-63.

9. Grande-Allen, K.J., et al., *Loss of chondroitin 6-sulfate and hyaluronan from failed porcine bioprosthetic valves.* J Biomed Mater Res A, 2003. **65**(2): p. 251-9.

10. Raghavan, D., D.T. Simionescu, and N.R. Vyavahare, *Neomycin prevents enzyme-mediated glycosaminoglycan degradation in bioprosthetic heart valves.* Biomaterials, 2007. **28**(18): p. 2861-8.

11. *Heart Disease Focus*. Retrieved May 2, 2007, from http://www.heartdisease focus.com/valvular-heart-disease/heart-valves.php.

12. *Heart and Vascular Guide*. Retrieved May 2, 2007, from http://www.clevelandclinic.org/heartcenter/pub/guide/heartworks/heartpics.htm.

13. Guyton, A.C. and J.E. Hall, *Textbook of Medical Physiology, 11th Edition.* 2005, Elsevier.

14. Christie, G.W., *Anatomy of aortic heart valve leaflets: the influence of glutaraldehyde fixation on function.* Eur J Cardiothorac Surg, 1992. **6 Suppl 1**: p. S25-32; discussion S33.

15. Schoen, F.J., *Aortic valve structure-function correlations: role of elastic fibers no longer a stretch of the imagination.* J Heart Valve Dis, 1997. **6**(1): p. 1-6.

16. Scott, M. and I. Vesely, *Aortic valve cusp microstructure: the role of elastin.* Ann Thorac Surg, 1995. **60**(2 Suppl): p. S391-4.

17. Scott, M.J. and I. Vesely, *Morphology of porcine aortic valve cusp elastin.* J Heart Valve Dis, 1996. **5**(5): p. 464-71.

18. Vesely, I. and D. Boughner, *Analysis of the bending behaviour of porcine xenograft leaflets and of neutral aortic valve material: bending stiffness, neutral axis and shear measurements.* J Biomech, 1989. **22**(6-7): p. 655-71.

19. Vesely, I. and R. Noseworthy, *Micromechanics of the fibrosa and the ventricularis in aortic valve leaflets.* J Biomech, 1992. **25**(1): p. 101-13.

20. Vesely, I., *The role of elastin in aortic valve mechanics.* J Biomech, 1998. **31**(2): p. 115-23.

21. Sauren, A.A., et al., *Aortic valve histology and its relation with mechanics-preliminary report.* J Biomech, 1980. **13**(2): p. 97-104.

22. Bashey, R.I., S. Torii, and A. Angrist, *Age-related collagen and elastin content of human heart valves.* J Gerontol, 1967. **22**(2): p. 203-8.

23. Mendelson, K. and F.J. Schoen, *Heart valve tissue engineering: concepts, approaches, progress, and challenges.* Ann Biomed Eng, 2006. **34**(12): p. 1799-819.

24. Talman, E.A. and D.R. Boughner, *Glutaraldehyde fixation alters the internal shear properties of porcine aortic heart valve tissue.* Ann Thorac Surg, 1995. **60**(2 Suppl): p. S369-73.

25. Talman, E.A. and D.R. Boughner, *Internal shear properties of fresh porcine aortic valve cusps: implications for normal valve function.* J Heart Valve Dis, 1996. **5**(2): p. 152-9.

26. Messier, R.H., Jr., et al., *Dual structural and functional phenotypes of the porcine aortic valve interstitial population: characteristics of the leaflet myofibroblast.* J Surg Res, 1994. **57**(1): p. 1-21.

27. Taylor, K.R. and R.L. Gallo, *Glycosaminoglycans and their proteoglycans: host-associated molecular patterns for initiation and modulation of inflammation.* Faseb J, 2006. **20**(1): p. 9-22.

28. Alberts, B., et al., *Molecular Biology of the Cell, 2nd Edition.* 1988, New York and London Garland Publishing, Inc.

29. Hascall, V.C. and G.K. Hascall, *Proteoglycans*, in *Cell biology of extracellular matrix* E.D. Hay, Editor. 1981, Plenum Publising Corporation.

30. Quinn, T.M., P. Dierickx, and A.J. Grodzinsky, *Glycosaminoglycan network geometry may contribute to anisotropic hydraulic permeability in cartilage under compression.* J Biomech, 2001. **34**(11): p. 1483-90.

31. Kanwar, Y.S., H. Makino, and F.A. Carone, *Basement membrane proteoglycans of the kidney.* Semin Nephrol, 1985. **5**(4): p. 307-13.

32. Heintz, B., et al., *Decreased glomerular basement membrane heparan sulfate proteoglycan in essential hypertension.* Hypertension, 1995. **25**(3): p. 399-407.

33. Raman, R., V. Sasisekharan, and R. Sasisekharan, *Structural insights into biological roles of protein-glycosaminoglycan interactions.* Chem Biol, 2005. **12**(3): p. 267-77.

34. Casu, B., et al., *Undersulfated and glycol-split heparins endowed with antiangiogenic activity.* J Med Chem, 2004. **47**(4): p. 838-48.

35. Sasisekharan, R., et al., *Roles of heparan-sulphate glycosaminoglycans in cancer.* Nat Rev Cancer, 2002. **2**(7): p. 521-8.

36. Carulli, D., et al., *Chondroitin sulfate proteoglycans in neural development and regeneration.* Curr Opin Neurobiol, 2005. **15**(1): p. 116-20.

37. Lyon, M., et al., *The interactions of hepatocyte growth factor/scatter factor and its NK1 and NK2 variants with glycosaminoglycans using a modified gel mobility shift assay. Elucidation of the minimal size of binding and activatory oligosaccharides.* J Biol Chem, 2004. **279**(42): p. 43560-7.

38. Liu, D., et al., *Mechanisms regulating the binding activity of CD44 to hyaluronic acid.* Front Biosci, 1998. **3**: p. d631-6.

39. Toole, B.P., T.N. Wight, and M.I. Tammi, *Hyaluronan-cell interactions in cancer and vascular disease.* J Biol Chem, 2002. **277**(7): p. 4593-6.

40. Simionescu, D.T., J.J. Lovekamp, and N.R. Vyavahare, *Degeneration of bioprosthetic heart valve cusp and wall tissues is initiated during tissue preparation: an ultrastructural study.* J Heart Valve Dis, 2003. **12**(2): p. 226-34.

41. Mori, Y. and A. Honda, *Glycosaminoglycans and proteoglycans of cardiac tissue: with special reference to cardiac valves,* in *Glycosaminoglycans and proteoglycans in physiological and pathological processes of body systems*, R. Varma and Editors. 1982: Switzerland.

42. Simionescu, D.T., J.J. Lovekamp, and N.R. Vyavahare, *Glycosaminoglycan-degrading enzymes in porcine aortic heart valves: implications for bioprosthetic heart valve degeneration.* J Heart Valve Dis, 2003. **12**(2): p. 217-25.

43. Torii, S., R.I. Bashey, and K. Nakao, *Acid mucopolysaccharide composition of human-heart valve.* Biochim Biophys Acta, 1965. **101**(3): p. 285-91.

44. Murata, K., *Acidic glycosaminoglycans in human heart valves.* J Mol Cell Cardiol, 1981. **13**(3): p. 281-92.

45. Torii, S. and R. Bashey, *High content of hyaluronic acid in normal human heart valves.* Nature, 1966. **209**(5022): p. 506-7.

46. Fraser, J.R., T.C. Laurent, and U.B. Laurent, *Hyaluronan: its nature, distribution, functions and turnover.* J Intern Med, 1997. **242**(1): p. 27-33.

47. Menzel, E.J. and C. Farr, *Hyaluronidase and its substrate hyaluronan: biochemistry, biological activities and therapeutic uses.* Cancer Lett, 1998. **131**(1): p. 3-11.

48. Sell, S. and R.E. Scully, *Aging Changes in the Aortic and Mitral Valves. Histologic and Histochemical Studies, with Observations on the Pathogenesis of Calcific Aortic Stenosis and Calcification of the Mitral Annulus.* Am J Pathol, 1965. **46**: p. 345-65.

49. Lovekamp, J.J., *Glycosaminoglycan function, instability, and preservation in bioprosthetic heart valves*, in *Bioengineering Dissertation*. 2005, Clemson University: Clemson, SC.

50. *Valvular Disease*, in *The US market for cardiovascular devices*. Retrieved May 20, 2007, from Kalorama Market Research Division http://www.kaloramainformation.com.

51. Rahimtoola, S.H. and R.L. Frye, *Valvular heart disease.* Circulation, 2000. **102**(20 Suppl 4): p. IV24-33.

52. Harken, D.E., et al., *Aortic valve replacement with a caged ball valve.* Am J Cardiol, 1962. **9**: p. 292-9.

53. Simionescu, D.T., *Artificial heart valves* in *Wiley's Encyclopedia of Biomedical Engineering*, M. Akay, Editor. 2006, John Wiley and Sons, Inc.: Hoboken, NJ.

54. Aslam, A.K., et al., *Prosthetic heart valves: Types and echocardiographic evaluation.* Int J Cardiol, 2007.

55. Bloomfield, P., *Choice of heart valve prosthesis.* Heart, 2002. **87**(6): p. 583-9.

56. DeWall, R.A., N. Qasim, and L. Carr, *Evolution of mechanical heart valves.* Ann Thorac Surg, 2000. **69**(5): p. 1612-21.

57. Butany, J., et al., *Mechanical heart valve prostheses: identification and evaluation (erratum).* Cardiovasc Pathol, 2003. **12**(6): p. 322-44.

58. *Prosthetic heart valves*, in *Mechanical heart valves*. Retrieved May 11, 2007, from http://cape.uwaterloo.ca/che100projects/heart/files/testing.htm.

59. Gott, V.L., D.E. Alejo, and D.E. Cameron, *Mechanical heart valves: 50 years of evolution.* Ann Thorac Surg, 2003. **76**(6): p. S2230-9.

60. Nair, K., C. Muraleedharan, and G. Bhuvaneshwar, *Developments in mechanical heart valve prosthesis.* Sadhana, 2003. **28**(3 & 4): p. 575-78.

61. *FDA Heart Health Online: prosthetic heart valves*, in *Recently approved prosthetic heart valves*. Retrieved May 3, 2007, from http://www.fda.gov/hearthealth/treatments/medicaldevices/prostheticheartvalve.html.

62. Datamonitor, *United States - Heart Valves*, in *Industry Profile*. 2006. p. 1-11.

63. Andersen, T.S., et al., *Intraoperative and postoperative evaluation of cavitation in mechanical heart valve patients.* Ann Thorac Surg, 2006. **81**(1): p. 34-41.

64. Schoen, F.J. and R.J. Levy, *Calcification of tissue heart valve substitutes: progress toward understanding and prevention.* Ann Thorac Surg, 2005. **79**(3): p. 1072-80.

65. Flanagan, T.C. and A. Pandit, *Living artificial heart valve alternatives: a review.* Eur Cell Mater, 2003. **6**: p. 28-45; discussion 45.

66. Grocott-Mason, R.M., et al., *Long-term results after aortic valve replacement in patients with congestive heart failure. Homografts vs prosthetic valves.* Eur Heart J, 2000. **21**(20): p. 1698-707.

67. Hawkins, J.A., et al., *Immunogenicity of decellularized cryopreserved allografts in pediatric cardiac surgery: comparison with standard cryopreserved allografts.* J Thorac Cardiovasc Surg, 2003. **126**(1): p. 247-52; discussion 252-3.

68. Palka, P., et al., *Primary aortic valve replacement with cryopreserved aortic allograft: an echocardiographic follow-up study of 570 patients.* Circulation, 2002. **105**(1): p. 61-6.

69. Grunkemeier, G.L. and E. Bodnar, *Comparison of structural valve failure among different 'models' of homograft valves.* J Heart Valve Dis, 1994. **3**(5): p. 556-60.

70. Zerbini, E.J., *Results of replacement of cardiac valves by homologous dura mater valves.* Chest, 1975. **67**(6): p. 706-10.

71. Puig, L.B., et al., *Four years experience with dura mater cardiac valves.* J Cardiovasc Surg (Torino), 1977. **18**(3): p. 247-55.

72. Puig, L.B., et al., *Homologous dura mater cardiac valves. Study of 533 surgical cases.* J Thorac Cardiovasc Surg, 1975. **69**(5): p. 722-8.

73. Ongcharit, C., et al., *Six years clinical experience with dura mater cardiac valves.* Thorac Cardiovasc Surg, 1983. **31**(5): p. 282-7.

74. Nuno-Conceicrao, A., et al., *Homologous dura mater cardiac valves. Structural aspects of eight implanted valves.* J Thorac Cardiovasc Surg, 1975. **70**(3): p. 499-508.

75. McGarvey, K.A., J.M. Lee, and D.R. Boughner, *Mechanical suitability of glycerol-preserved human dura mater for construction of prosthetic cardiac valves.* Biomaterials, 1984. **5**(2): p. 109-17.

76. Manothaya, C., et al., *Homologous dura mater cardiac valves.* J Med Assoc Thai, 1977. **60**(11): p. 545-50.

77. Allen, D.J., et al., *Evidence of remodeling in dura mater cardiac valves.* J Thorac Cardiovasc Surg, 1982. **84**(2): p. 267-81.

78. Vesely, I., *The evolution of bioprosthetic heart valve design and its impact on durability.* Cardiovasc Pathol, 2003. **12**(5): p. 277-86.

79. Sapirstein, J.S. and P.K. Smith, *The "ideal" replacement heart valve.* Am Heart J, 2001. **141**(5): p. 856-60.

80. *Heart Valve Diseases*, in *My heart: conditions*. Retrieved May 11th, 2007, from http://www.lifeisnow.com/MyHeart/Conditions.aspx.

81. Luciani, G.B., *Stentless aortic valve replacement: current status and future trends.* Expert Rev Cardiovasc Ther, 2004. **2**(1): p. 127-40.

82. Borger, M.A., et al., *Stentless aortic valves are hemodynamically superior to stented valves during mid-term follow-up: a large retrospective study.* Ann Thorac Surg, 2005. **80**(6): p. 2180-5.

83. Woodroof, E.A., *Use of glutaraldehyde and formaldehyde to process tissue heart valves.* J Bioeng, 1978. **2**(1-2): p. 1-9.

84. Broom, N.D. and F.J. Thomson, *Influence of fixation conditions on the performance of glutaraldehyde-treated porcine aortic valves: towards a more scientific basis.* Thorax, 1979. **34**(2): p. 166-76.

85. Broom, N.D. and D. Marra, *Effect of glutaraldehyde fixation and valve constraint conditions on porcine aortic valve leaflet coaptation.* Thorax, 1982. **37**(8): p. 620-6.

86. Gudbjartsson, T., S. Aranki, and L.H. Cohn, *Mechanical/bioprosthetic mitral valve replacement*, in *Cardiac Surgery in the Adult*, L.H. Cohn and L.H. Edmunds, Jr., Editors. 2003, McGraw-Hill: New York. p. 951-986.

87. Jayakrishnan, A. and S.R. Jameela, *Glutaraldehyde as a fixative in bioprostheses and drug delivery matrices.* Biomaterials, 1996. **17**(5): p. 471-84.

88. Simionescu, D.T., *Prevention of calcification in bioprosthetic heart valves: challenges and perspectives.* Expert Opin Biol Ther, 2004. **4**(12): p. 1971-85.

89. Sellaro, T.L., et al., *Effects of collagen fiber orientation on the response of biologically derived soft tissue biomaterials to cyclic loading.* J Biomed Mater Res A, 2007. **80**(1): p. 194-205.

90. Wells, S.M., T. Sellaro, and M.S. Sacks, *Cyclic loading response of bioprosthetic heart valves: effects of fixation stress state on the collagen fiber architecture.* Biomaterials, 2005. **26**(15): p. 2611-9.

91. Mirnajafi, A., et al., *The flexural rigidity of the aortic valve leaflet in the commissural region.* J Biomech, 2006. **39**(16): p. 2966-73.

92. Song, T., I. Vesely, and D. Boughner, *Effects of dynamic fixation on shear behaviour of porcine xenograft valves.* Biomaterials, 1990. **11**(3): p. 191-6.

93. Jamieson, W.R., et al., *Carpentier-Edwards standard porcine bioprosthesis: a 21-year experience.* Ann Thorac Surg, 1998. **66**(6 Suppl): p. S40-3.

94. Butany, J. and R. Leask, *The failure modes of biological prosthetic heart valves.* J Long Term Eff Med Implants, 2001. **11**(3-4): p. 115-35.

95. Valente, M., et al., *Heart valve bioprosthesis durability: a challenge to the new generation of porcine valves.* Eur J Cardiothorac Surg, 1992. **6 Suppl 1**: p. S82-90.

96. Zilla, P., P. Human, and D. Bezuidenhout, *Bioprosthetic heart valves: the need for a quantum leap.* Biotechnol Appl Biochem, 2004. **40**(Pt 1): p. 57-66.

97. Giachelli, C.M., *Vascular calcification mechanisms.* J Am Soc Nephrol, 2004. **15**(12): p. 2959-64.

98. Nimni, M.E., et al., *Factors which affect the calcification of tissue-derived bioprostheses.* J Biomed Mater Res, 1997. **35**(4): p. 531-7.

99. Girardot, M.N., et al., *Role of glutaraldehyde in calcification of porcine heart valves: comparing cusp and wall.* J Biomed Mater Res, 1995. **29**(7): p. 793-801.

100. Kim, K.M., *Cells, rather than extracellular matrix, nucleate apatite in glutaraldehyde-treated vascular tissue.* J Biomed Mater Res, 2002. **59**(4): p. 639-45.

101. Vyavahare, N., et al., *Prevention of bioprosthetic heart valve calcification by ethanol preincubation. Efficacy and mechanisms.* Circulation, 1997. **95**(2): p. 479-88.

102. Rao, K.P. and C. Shanthi, *Reduction of calcification by various treatments in cardiac valves.* J Biomater Appl, 1999. **13**(3): p. 238-68.

103. Stacchino, C., et al., *Detoxification process for glutaraldehyde-treated bovine pericardium: biological, chemical and mechanical characterization.* J Heart Valve Dis, 1998. **7**(2): p. 190-4.

104. Hunter, G.K., *Role of proteoglycan in the provisional calcification of cartilage. A review and reinterpretation.* Clin Orthop Relat Res, 1991(262): p. 256-80.

105. Hunter, G.K. and C.A. Weinert, *Inhibition of proteoglycan biosynthesis decreases the calcification of chondrocyte cultures.* Connect Tissue Res, 1996. **35**(1-4): p. 379-84.

106. Bailey, M.T., et al., *Role of elastin in pathologic calcification of xenograft heart valves.* J Biomed Mater Res A, 2003. **66**(1): p. 93-102.

107. Sacks, M.S. and F.J. Schoen, *Collagen fiber disruption occurs independent of calcification in clinically explanted bioprosthetic heart valves.* J Biomed Mater Res, 2002. **62**(3): p. 359-71.

108. Ikhumetse, J.D., et al., *Cyclic aortic pressure affects the biological properties of porcine pulmonary valve leaflets.* J Heart Valve Dis, 2006. **15**(2): p. 295-302.

109. Englberger, L., et al., *Importance of implant technique on risk of major paravalvular leak (PVL) after St. Jude mechanical heart valve replacement: a report from the Artificial Valve Endocarditis Reduction Trial (AVERT).* Eur J Cardiothorac Surg, 2005. **28**(6): p. 838-43.

110. Bender, J.R., *Heart valve disease*, in *Major cardiovascular disorders*, J.R. Bender, Editor. 1992, Yale University School of Medicine.

111. Butany, J.W., et al., *Infective endocarditis in a hancock bioprosthetic heart valve.* J Card Surg, 2005. **20**(4): p. 389-92.

112. El-Ahdab, F., et al., *Risk of endocarditis among patients with prosthetic valves and Staphylococcus aureus bacteremia.* Am J Med, 2005. **118**(3): p. 225-9.

113. Mestres, C.A. and J.M. Miro, *Allograft aortic root replacement in complex prosthetic valve endocarditis.* Eur J Cardiothorac Surg, 2007.

114. Human, P. and P. Zilla, *Inflammatory and immune processes: the neglected villain of bioprosthetic degeneration?* J Long Term Eff Med Implants, 2001. **11**(3-4): p. 199-220.

115. Human, P. and P. Zilla, *Characterization of the immune response to valve bioprostheses and its role in primary tissue failure.* Ann Thorac Surg, 2001. **71**(5 Suppl): p. S385-8.

116. Mecozzi, G., et al., *Intravascular hemolysis in patients with new-generation prosthetic heart valves: a prospective study.* J Thorac Cardiovasc Surg, 2002. **123**(3): p. 550-6.

117. Sun, W., A. Abad, and M.S. Sacks, *Simulated bioprosthetic heart valve deformation under quasi-static loading.* J Biomech Eng, 2005. **127**(6): p. 905-14.

118. Sun, W., et al., *Response of heterograft heart valve biomaterials to moderate cyclic loading.* J Biomed Mater Res A, 2004. **69**(4): p. 658-69.

119. Sun, W., et al., *Biaxial mechanical response of bioprosthetic heart valve biomaterials to high in-plane shear.* J Biomech Eng, 2003. **125**(3): p. 372-80.

120. Vesely, I., *A mechanism for the decrease in stiffness of bioprosthetic heart valve tissues after cross-linking.* Asaio J, 1996. **42**(6): p. 993-9.

121. Thubrikar, M.J., et al., *Stress analysis of porcine bioprosthetic heart valves in vivo.* J Biomed Mater Res, 1982. **16**(6): p. 811-26.

122. Farndale, R.W., D.J. Buttle, and A.J. Barrett, *Improved quantitation and discrimination of sulphated glycosaminoglycans by use of dimethylmethylene blue.* Biochim Biophys Acta, 1986. **883**(2): p. 173-7.

123. Farndale, R.W., C.A. Sayers, and A.J. Barrett, *A direct spectrophotometric microassay for sulfated glycosaminoglycans in cartilage cultures.* Connect Tissue Res, 1982. **9**(4): p. 247-8.

124. Hoemann, C.D., et al., *A multivalent assay to detect glycosaminoglycan, protein, collagen, RNA, and DNA content in milligram samples of cartilage or hydrogel-based repair cartilage.* Anal Biochem, 2002. **300**(1): p. 1-10.

125. Pieper, J.S., et al., *Preparation and characterization of porous crosslinked collagenous matrices containing bioavailable chondroitin sulphate.* Biomaterials, 1999. **20**(9): p. 847-58.

126. Salmen, S., et al., *Sulphated oligosaccharides as inhibitors of hyaluronidases from bovine testis, bee venom and Streptococcus agalactiae.* Planta Med, 2005. **71**(8): p. 727-32.

127. Zhong, S.P., et al., *Biodegradation of hyaluronic acid derivatives by hyaluronidase.* Biomaterials, 1994. **15**(5): p. 359-65.